JOURNAL OF GEOPHYSICAL RESEARCH, VOL. 113, D11208, doi:10.1029/2007JD009588, 2008

Coupling and evaluating gas/particle mass transfer treatments for aerosol simulation and forecast

Xiao-Ming Hu,[1] Yang Zhang,[1] Mark Z. Jacobson,[2] and Chak K. Chan[3]

Received 11 November 2007; revised 27 December 2007; accepted 21 February 2008; published 12 June 2008.

[1] Simulating gas/particle mass transfer in three-dimensional (3-D) air quality models (AQMs) represents one of the major challenges for both hindcasting and forecasting. The lack of an efficient yet accurate gas/particle mass transfer treatment for aerosol simulation and forecast in 3-D AQMs warrants its development, improvement, and evaluation. In this paper, several condensation/evaporation schemes (e.g., the Bott, Trajectory-Grid (T-G), Walcek, and analytical predictor of condensation (APC)) are first tested in a condensation-only case. The APC and Walcek schemes are shown to be more accurate than the Bott and T-G schemes. The Walcek and the APC schemes are then incorporated into the Model of Aerosol Dynamics, Reaction, Ionization, and Dissolution (MADRID) to solve the gas/particle mass transfer process explicitly. The test simulations with MADRID are initialized with measurements available from three sites with representative meteorological and emission characteristics. The results are evaluated using benchmark based on the kinetic approach with 500-section for all cases and available measurements from two sites. The box MADRID tests have shown that the bulk equilibrium approach fails to predict the distribution of semivolatile species (e.g., ammonium, chloride, and nitrate) because of the equilibrium and internal mixture assumptions. The hybrid approach exhibits the same problem for some cases as the bulk equilibrium approach since it assumes bulk equilibrium for fine particles. The kinetic approaches (including the APC and Walcek schemes for the condensation/evaporation equations) predict the most accurate solutions. Among all approaches tested, the bulk equilibrium approach is the most computationally efficient, and the kinetic/Walcek scheme provides an accurate solution but is the slowest due to its requirement for a small time step. Overall, the kinetic/APC and hybrid/APC schemes are attractive for 3-D applications in terms of both accuracy and computational efficiency.

Citation: Hu, X.-M., Y. Zhang, M. Z. Jacobson, and C. K. Chan (2008), Coupling and evaluating gas/particle mass transfer treatments for aerosol simulation and forecast, *J. Geophys. Res.*, *113*, D11208, doi:10.1029/2007JD009588.

1. Introduction

[2] Modeling the size/composition distribution of atmospheric aerosols is important for assessing the impacts of human activities on air quality and climate change. Simulating gas/particle mass transfer is essential for accurately predicting aerosol size/composition distributions since secondary aerosol (SA) accounts for a significant fraction of total aerosol mass. Often most of the mass of particulate matter with aerodynamic diameters equal to or less than 2.5 μm ($PM_{2.5}$) is composed of SA [*Wexler et al.*, 1994], in some cases more than 90% of the $PM_{2.5}$ mass may be attributed to SA [*Plessow et al.*, 2005]. The treatment of SA, however, in three-dimensional (3-D) air quality models (AQMs) represents one of the major challenges for hindcasting and forecasting air quality.

[3] Three main approaches (i.e., equilibrium, kinetic (or dynamic), and hybrid) have been used to simulate gas/particle mass transfer in AQMs. The equilibrium approach assumes equilibrium between bulk gas and liquid/solid phases and can be divided further into bulk and size-resolved equilibrium approaches. In the bulk equilibrium approach, the same chemical composition is assumed for all particles over all size ranges (i.e., internal mixture) and a thermodynamic model (e.g., ISORROPIA [*Nenes et al.*, 1998]) is typically used to calculate equilibrium bulk gas and particle concentrations. The bulk equilibrium approach has been widely used in 3-D AQM applications [*Russell et al.*, 1983, 1988; *Pilinis et al.*, 1987; *Binkowski and Shankar*, 1995; *Lurmann et al.*, 1997; *Binkowski and Roselle*, 2003; *Zhang et al.*, 2004; *Gaydos et al.*, 2007] because of its computational efficiency. These models either assume mono-disperse aerosols or use bulk equilibrium with redistribution of the bulk material to different particle sizes

[1]Department of Marine, Earth and Atmospheric Sciences, North Carolina State University, Raleigh, North Carolina, USA.
[2]Department of Civil and Environmental Engineering, Stanford University, Stanford, California, USA.
[3]Department of Chemical Engineering, Hong Kong University of Science and Technology, Kowloon, Hong Kong, China.

0148-0227/08/2007JD009588$09.00

following the equilibrium calculation [*Pandis et al.*, 1993; *Lurmann et al.*, 1997; *Capaldo et al.*, 2000; *Zhang et al.*, 2004; *Debry et al.*, 2007]. Both methods neglect the differences in chemical driving forces for different aerosol sections (or bins) by assuming an internal mixture with a potential mixing of acidic particles with alkaline particles that may introduce errors [*Ansari and Pandis*, 1999; *Moya et al.*, 2001; *Kerminen et al.*, 2001; *Myhre et al.*, 2006]. In other words, the calculation of composition in each section is not based on the thermodynamic properties of that section. Instead, it is based on the thermodynamic computation of the bulk liquid/solid phases. Size-resolved equilibrium simulates equilibrium between bulk gas phase and individual size sections [e.g., *Pilinis and Seinfeld*, 1987; *Moya et al.*, 2002], without assuming an internal mixture over the entire size range. It, however, may not have a unique solution in some cases (e.g., a solid forms from two gases (e.g., NH_4NO_3(s) or NH_4Cl(s))) [*Wexler and Seinfeld*, 1990; *Jacobson*, 1999]. Both the bulk and size-resolved equilibrium approaches rely on the instantaneous bulk equilibrium assumption that may be invalid under some atmospheric conditions (e.g., under conditions with high coarse particle concentrations and cold temperatures) [*Wexler and Seinfeld*, 1990; *Zhang et al.*, 1999]. The kinetic approach [e.g., *Meng and Seinfeld*, 1996; *Jacobson*, 1997a, 1997b; *Meng et al.*, 1998; *Sun and Wexler*, 1998; *Pilinis et al.*, 2000] simulates explicit mass transfer to each section. Since no equilibrium assumptions are made and the chemical driving force may vary with size sections, this approach provides the most accurate solution when an appropriate numerical solver and a sufficiently fine size resolution are used. However, its computational demands hinder its wide applications in 3-D AQMs. Existing kinetic approaches are applied primarily in box models [e.g., *Meng and Seinfeld*, 1996; *Pilinis et al.*, 2000] although there exist a few 3-D applications for episodes of a few days [e.g., *Meng et al.*, 1998]. *Jacobson* [2005] developed the Predictor of Nonequilibrium Growth (PNG)-EQUISOLV II scheme to reduce the computational cost of the kinetic mass transfer treatment, which has not been used for most 3-D AQMs. The hybrid approach provides a compromise between accuracy and efficiency by using equilibrium approach for fine particles and kinetic approach for coarse particles; but uncertainties exist in the selection of the cutoff size (i.e., threshold diameter) between the two approaches and it has only been tested with limited episodes [e.g., *Capaldo et al.*, 2000; *Koo et al.*, 2003; *Gaydos et al.*, 2003; *Tombette and Sportisse*, 2007]. The lack of an efficient yet accurate gas/particle kinetic mass transfer treatment for aerosol simulation and forecast in 3-D AQMs warrants its development, improvement, and evaluation. In addition, the above approaches have seldom been evaluated using observational data largely due to the lack of such data for rigorous testing of those model treatments.

[4] In this work, several condensation/evaporation schemes are first tested using a hypothetical case as stand alone schemes and then incorporated into the kinetic approach in a box aerosol model (i.e., The Model of Aerosol Dynamics, Reaction, Ionization, and Dissolution (MADRID) [*Zhang et al.*, 2004]) to explicitly simulate gas/particle mass transfer. The existing kinetic and hybrid approaches for gas/particle mass transfer in MADRID are improved and tested along with two existing equilibrium approaches using available observational data at representative locations. MADRID uses a sectional representation with any size resolution at the user's choice [*Zhang et al.*, 2004]. It simulates all major aerosol processes except for coagulation. For gas/particle mass transfer testing, nucleation is turned off so that the effects of different condensation schemes in the kinetic approach can be isolated and examined. Other processes such as photochemistry, transport, and deposition are not treated in the MADRID box model. Emissions, however, are implicitly treated in the applications of MADRID for some cases (see section 3.1). The use of such a stand alone aerosol box model follows a classic approach of studying chemical kinetics; it permits an isolation of major aerosol processes from other processes, which is necessary for a mechanistic study of gas/particle mass transfer process. This is because, when other processes are included in testing gas/particle mass transfer approaches, many factors and feedbacks will come into play that can distort the model results regarding gas/particle mass transfer approaches, making it impossible to judge if good results from a gas/particle mass transfer approach are due simply to its treatments or to different effects of meteorology on simulated concentrations in one simulation versus another.

[5] Similar approaches have been widely used to study gas/particle partitioning equilibrium [e.g., *Pilinis and Seinfeld*, 1987; *Hayami and Carmichael*, 1997; *Ansari and Pandis*, 1999; *Jacobson*, 1999; *Moya et al.*, 2001, 2002; *Fridlind and Jacobson*, 2000; *Fridlind et al.*, 2000; *Campbell et al.*, 2002; *Zhang et al.*, 2002; *Trebs et al.*, 2005; *Yao et al.*, 2006; *Dasgupta et al.*, 2007; *Goetz et al.*, 2008]. In contrast, our cases involve nonequilibrium gas/particle mass transfer. The strengths and limitations of each condensation scheme and each gas/particle mass transfer approach are identified and analyzed. The approach that provides the best compromise between accuracy and efficiency will be recommended for further testing and application in 3-D AQMs.

2. Aerosol Condensation and Evaporation Schemes

2.1. Description of Various Schemes

[6] The kinetic gas/particle mass transfer approach solves the following condensation/evaporation equation explicitly:

$$\frac{\partial p_1}{\partial t} = G_i - R_i = H_i p - \frac{1}{3}\frac{\partial H p_1}{\partial \mu} \tag{1}$$

where G_i and R_i denote the growth and redistribution terms, respectively. P_i is the mass distribution of species i, H_i is the mass transfer rate of species i, μ is the log of the diameter of the particle, p is the total mass concentration, and H is the total mass transfer rate. The G_i and R_i terms can be solved by means of operator splitting because the growth process occurs on a faster scale than the scale over which they shift [*Sun and Wexler*, 1998].

[7] The redistribution term, R_i, is mathematically similar to the advection term; it can be solved with three major numerical techniques: Lagrangian, Eulerian, and moving-center [*Seigneur*, 2001; *Zhang et al.*, 2004]. The Lagrangian approach (also referred to as the full-moving approach, e.g., *Chock et al.* [1996, 2005], *Chock and Winkler* [2000], and

Table 1. The Numerical Condensation Schemes Tested in This Work

Condensation Schemes	Redistribution Term	Growth Term
T-G	Lagrangian approach (T-G)	forward Euler method
Bott; Walcek	Eulerian approaches (Bott; Walcek)	forward Euler method
APC_MC	moving-center approach	mass-conserving, noniterative analytical solution
APC_FM	Lagrangian approach	mass-conserving, noniterative analytical solution

Jacobson [1997a]) uses a moving-sectional method to simulate the growth/shrinkage of the particle mass along the size coordinate. Interpolation is needed to obtain a fixed-grid distribution when the Lagrangian approach is applied with other processes (e.g., nucleation, transport) [*Debry et al.*, 2007]. In such a case the Lagrangian approach becomes a semi-Lagrangian approach. The interpolation may introduce some errors that may be propagated into the model predictions. The semi-Lagrangian approach may therefore not conserve mass. Eulerian approaches [e.g., *Bott*, 1989; *Walcek and Aleksic*, 1998; *Walcek*, 2000; *Nguyen and Dabdub*, 2002] calculate the mass flux between the adjacent sections using a fixed-grid size representation. The Eulerian approach is of advantage because of mass conservation upon satisfaction of the Courant criterion, but it requires a small time step to satisfy this criterion. The moving-center approach [e.g., *Jacobson*, 1997a] uses fixed size bin boundaries but allows the mean diameter of particles to vary within the size bin. It has nearly the same accuracy as the full-moving approach while retaining the advantage of being able to couple with the treatments of coagulation, nucleation, emission, and transport of particles since the size bin structures do not change from time to time or location to location. However, numerical diffusion may still occur during growth, transport, or size-averaging processes.

[8] The growth term, G_i, can be solved by several methods. For example, forward Euler method [*Dhaniyala and Wexler*, 1996; *Sun and Wexler*, 1998; *Chock and Winkler*, 2000; *Nguyen and Dabdub*, 2002; *Gaydos et al.*, 2003], which assumes constant condensation rates during the integration time step and requires the use of a small time step. Some other ordinary differential equations (ODE) solvers (e.g., Sparse-Matrix Vectorized Gear Code (SMVGEAR) II [*Jacobson*, 1995], Livermore Solver for Ordinary Differential Equations (LSODE), the variable coefficient ODE solver (DVODE)) are used to solve the ODE system composed of G_i for each aerosol size section and each aerosol species and the mass conservation equation for the gas species [*Jacobson*, 1997b; *Pilinis et al.*, 2000]. Iterations are needed for the solvers to obtain a solution. *Jacobson* [1997b] introduced a noniterative, unconditionally stable analytical predictor of condensation (APC) to solve the growth term which allows the use of a larger time step (up to 15 s) without sacrifice of accuracy.

[9] In the aerosol module, condensation schemes need to be coupled with an equilibrium solver to compute the condensation rate, which is computationally expensive. The computational efficiency of condensation scheme itself thus does not play an important role in the aerosol condensation and evaporation calculation since the computational time is dominated by the equilibrium solver [*Wexler et al.*, 1994]. The time step allowed by the condensation schemes, however, makes the difference for the computational cost of this calculation. The use of a larger time step (i.e., time interval between growth and equilibrium) in the APC scheme reduces the times to invoke an equilibrium solver, which speeds up the aerosol calculations.

2.2. Evaluation of Stand Alone Condensation Schemes

[10] In this work, the stand alone condensation/evaporation schemes (without coupling to an equilibrium solver) are first tested for a simple case, in which sulfuric acid (H_2SO_4) is the only condensing species. Since the saturation vapor pressure of sulfuric acid is negligible, it is assumed to be zero. The condensation schemes tested include the Bott, the Chock (or Trajectory-Grid (T-G)), the Walcek, and the APC schemes. The methods for solving growth and redistribution equations used in the five schemes are summarized in Table 1.

[11] The Bott scheme is a high order accurate, positive definite scheme [*Bott*, 1989] that has been used widely for solving advection equations. The T-G scheme assigns the spatial locations of points on a given concentration profile to a set of concentration pulses; then tracks the pulses as they undergo growth/shrinkage [*Chock et al.*, 1996; *Chock and Winkler*, 2000]. It is more accurate than the Bott scheme for the condensation test [*Hu et al.*, 2005]. The Walcek scheme uses a second-order accurate, upstream approximation with monotone limiters and adjusts fluxes at two cell edges around local extremes, which is shown to be more accurate and more computationally efficient than the fourth-order Bott scheme [*Walcek*, 2000]. The Bott, T-G, and Walcek schemes use the forward Euler method to solve the growth term in the condensation equation. They differ in terms of redistribution methods with a semi-Lagrangian approach for the T-G scheme and an Eulerian approach for the Bott and Walcek schemes. APC uses a mass-conserving, noniterative analytical solution to a discretized form of the growth/evaporation equation between the gas phase and multiple size bins. Two methods are used to solve the redistribution equation: moving-center and full-moving approaches (referred to as APC_MC and APC_FM, respectively).

[12] The test case is taken from *Seigneur et al.* [1986] and *Zhang et al.* [1999] for the hazy conditions with an H_2SO_4 condensation rate of 5.5 μm^3 cm^{-3} 12 h^{-1}. 12 sections are used for all schemes in the test simulations. Two pulses are used in each section for the T-G scheme. Figure 1 shows predictions from the Bott, T-G, Walcek, APC_MC, and APC_FM schemes. The "exact" solution, obtained with the APC_FM scheme with 500 sections by *Zhang et al.* [1999] shows two distinct modes, one centered at 0.09 μm, and one centered at 0.21 μm. Compared with the "exact" solution, the Bott scheme is significantly diffusive in the ultrafine sections (so-called upstream diffusion). The T-G scheme with a total of 12 bins and two pulses per bin is also diffusive, overpredicting the concentration for the bin centered at 0.07 μm. The Walcek and APC schemes are much less diffusive than the Bott and T-G schemes in this case. The distinct nuclei mode in the "exact" solution is nearly replicated by the APC_FM scheme, but not so well by the APC_MC scheme with 12 bins. While the APC_FM scheme simulates well the two bins bounding the peak of

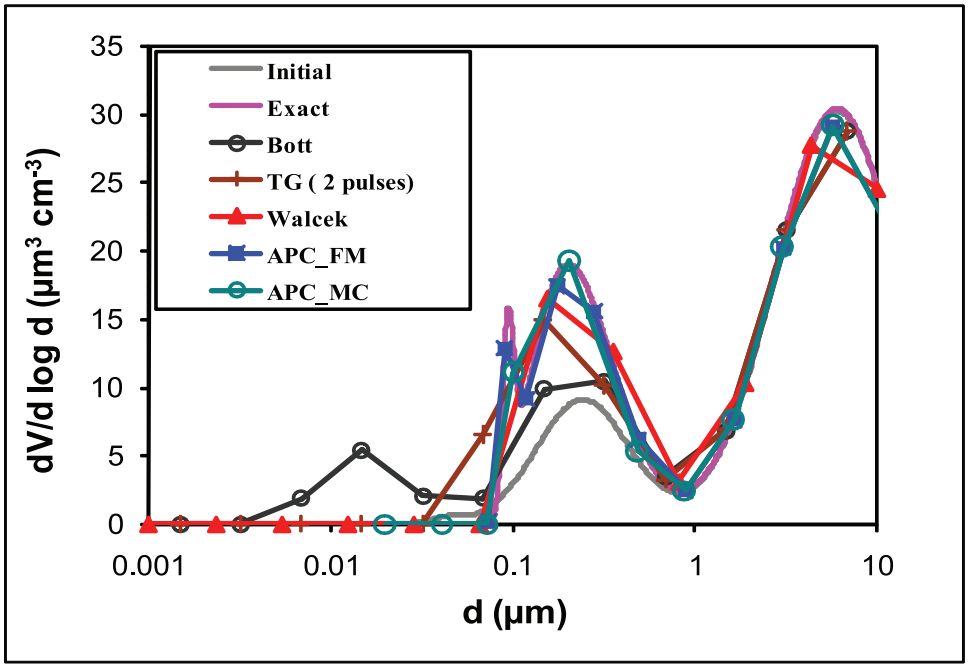

Figure 1. Simulations of condensation for hazy conditions with a condensation rate of 5.5 μm^3 cm^{-3} per 12-h using different condensation schemes: The Bott, T-G, Walcek, APC_MC, and APC_FM schemes, where APC_MC and APC_FM denote the APC scheme with the moving-center and full-moving approaches for redistribution.

the accumulation mode (at 0.21 μm) of the "exact" solution, the APC_MC scheme reproduces the peak of the accumulation mode better than the APC_FM scheme, as a result of averaging diameters of particles from adjacent bins around the peak. When other size resolutions are used (e.g., 8 or 16 size sections), averaging diameters of adjacent bins does not always yield a good agreement with the peak of the accumulation mode, and in such cases the APC_FM scheme gives a closer agreement to the peak than the APC_MC scheme (figures not shown). A more quantitative method of evaluation is to calculate the normalized mean error (NME) over the diameter range of 0.01–2.15 μm following the approach of *Zhang et al.* [1999]. The NMEs are 41.7, 15.1, 20.0, 8.3, and 11.1% for the Bott, T-G, Walcek, APC_FM, and APC_MC, respectively, when 12 sections are used. Among the five condensation schemes tested using a 12-section resolution, the APC_FM, APC_MC, and Walcek schemes give overall best predictions in terms of both simulated size distribution and NMEs. The T-G scheme gives a smaller NME than that of the Walcek scheme, but it is subject to upstream numerical diffusion in the size range of 0.05–0.1 μm. The Bott scheme gives less accurate performance.

[13] To examine the sensitivity of predictions to the total number of the sections and pulses used, additional simulations are conducted with the APC_FM using 8 and 30 size sections and with T-G schemes using 12 size sections with 4 pulses per section and 30 size sections with 2 and 4 pulses per section for the T-G scheme (Figure 2). Compared with results with 12 sections, the APC_FM scheme with 8 sections predicts better the peak of the accumulation mode but completely misses the narrow nucleation mode, whereas the use of 30 sections can reproduce precisely the aerosol size distribution of the "exact" solution. The CPU increases less than linearly (0.038, 0.054, and 0.118 s for simulations with 8, 12, and 30 sections, respectively) when the total number of sections increases from 8 to 30. For the T-G scheme with 2 pulses per section, increasing the total number of sections from 12 to 30 gives a better prediction for the nuclei mode but still fails to replicate fully the narrow peak of this mode. While increasing pulses from 2 to 4 per section at a size resolution of 12 sections shows no improvement, it greatly improves the prediction for the narrow nuclei mode with slight numerical diffusion at a size resolution of 30 sections. Those results indicate that the pulse resolution in the T-G scheme is more critical than the size resolution at a higher size resolution under the test condition. Compared with the T-G scheme with 12 sections and 2 pulses per section, the CPU time increases by 1.18 s (4.4%) when increasing pulse resolution alone to 4 pulses, by 37.9 s (142.4%) when increasing size resolution alone to 30 sections, and by 40.7 s (153.2%) when increasing both size and pulse resolutions for the T-G scheme.

[14] In addition to a relatively poor performance in the condensation test, the kinetic mass transfer approaches with the Bott and T-G schemes also require small time steps (e.g., 0.5 s) with a CPU two orders of magnitude higher than the equilibrium approach in the box model with a hypothetical test case for gas/particle mass transfer of *Zhang et al.* [1999] [*Hu et al.*, 2005], which is not desirable for most 3-D applications. The APC_MC scheme, on the other hand, may be a better candidate for 3-D applications; it is therefore further tested in the kinetic approach in MADRID using available observations. The Walcek scheme also takes similar CPU to that of the Bott and T-G schemes, but it is the most accurate scheme among those that require a small

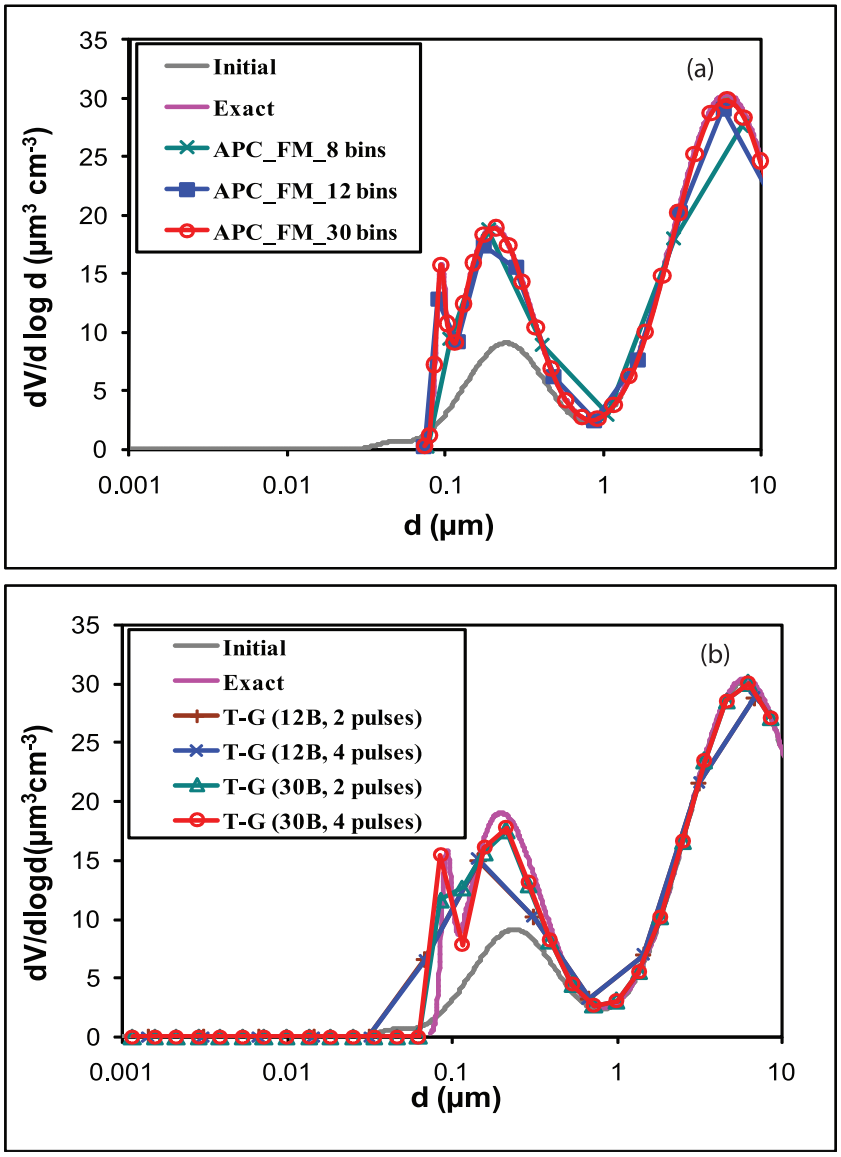

Figure 2. Sensitivity of (a) the APC_FM scheme to the aerosol size resolution and (b) trajectory-grid (T-G) scheme to the aerosol size resolution and pulses used in each bin for the same test case as for Figure 1.

time step tested here. It is therefore also selected for the gas/particle mass transfer testing.

3. Gas/Particle Mass Transfer Approaches

[15] The existing kinetic approach in MADRID uses the Bott scheme for condensation/evaporation. It is not operational in 3-D applications because of its high CPU cost. In this work, the Walcek and APC_MC condensation schemes have been implemented into MADRID to replace Bott's scheme in the kinetic approach to explicitly solve condensation/evaporation during the gas/particle mass transfer process (referred to as kinetic/Walcek and kinetic/APC_MC, respectively). Both schemes are coupled with an aerosol thermodynamic model (i.e., the latest version (v1.7) of ISORROPIA of *Nenes et al.* [1999]) in MADRID, which predicts the physical state of the particles (i.e., liquid or solid) and computes the surface vapor pressure of species given aerosol composition if the particles are wet. The surface vapor pressure is used to calculate the condensation/evaporation rate at every time step. For dry particles, the condensation/evaporation rates are computed based on the method of *Pilinis et al.* [2000] that uses the electroneutrality constraints to simulate the species flux to solid particles. The original CMU hybrid scheme in MADRID assumes bulk equilibrium for the first 6 sections and uses DVODE to solve the gas/particle mass transfer for the coarse mode explicitly [*Capaldo et al.*, 2000]. In this work, the APC_MC scheme is incorporated as an alternative to DVODE in the hybrid approach (referred to as the modified CMU hybrid/APC_MC), which is tested with threshold diameters of 1.0 and 2.15 μm (assuming bulk equilibrium for the first 5 and 6 sections, respectively).

[16] The gas/particle mass transfer approaches tested in this work include two existing equilibrium approaches: the California Institute of Technology (CIT) and Carnegie Mellon University (CMU) bulk equilibrium approaches (referred to as CIT and CMU bulk equilibrium approaches, respectively), two new kinetic approaches: kinetic/Walcek and kinetic/APC_MC, and one hybrid approach: the modified CMU hybrid/APC_MC. The CIT and CMU equilibrium approaches are both bulk equilibrium approaches, which assume that the liquid and/or solid phases, as a whole, are in equilibrium with the gas phase. They differ in terms of their methods to allocate the increase (or decrease in case of evaporation) of mass concentrations to different size sections: the former is based on the initial sulfate mass distribution [*Zhang et al.*, 2004], while the latter is based on weighting factors that depend largely on aerosol surface area [*Capaldo et al.*, 2000]. While no condensational growth law is used for mass allocation in the CIT approach, the weighting factors for mass allocation in the CMU approach are calculated based on condensational growth law using a diffusion-limited assumption. In both approaches, the mass allocation over different size sections may cause nonequilibrium between each section and the gas phase although the bulk liquid and/or solid phases, as a whole, are assumed to be in equilibrium with gas phase.

3.1. Test of Gas/Particle Mass Transfer Approaches in MADRID

[17] The aforementioned gas/particle mass transfer approaches are evaluated in box MADRID with several observational data sets, including those for Hong Kong (HK) [*Yao et al.*, 2001], Tampa Bay (TB) [*Evans and Poor*, 2001; *Campbell et al.*, 2002], and California Regional $PM_{10}/PM_{2.5}$ Air Quality Study (CRPAQS) [*Chow et al.*, 2006a, 2006b]. Those simulations are conducted using eight size sections. While data are available for model initialization and evaluation for the HK and CRPAQS test cases, they are only available for model initialization for the TB case. Simulations with the kinetic/APC_MC and the kinetic/Walcek at a high size resolution of 500-section and a short time step of 0.5 s are also conducted to develop benchmarks to evaluate different gas/particle mass transfer approaches, which will be particularly useful for the cases without observations for model evaluation (e.g., the TB case). The initial size distribution with 500 sections is obtained by evenly distributing the observed 8-section initial distribution into the corresponding sections in the 500-section size structure. Although the aerosol measurements may contain some sea-salt sulfate, sea-salt sulfate is not treated in box MADRID because of its relatively small mass fractions at those sites. In addition, the Web version of HYSPLIT trajectory model of *Draxler and Rolph* [2003] is used separately to perform back trajectory analyses based on the FNL data set (known as the Final Run at National Centers for Environmental Prediction (NCEP)) at three sites to identify the origin of the air mass arriving at these sites in order to understand the sources of aerosols and their precursors.

[18] During spring, HK is mostly affected by clean marine air mass; sea salt is the dominant source of the particles while regional pollution also plays a role [*Yao et al.*, 2001; *Pathak et al.*, 2003; *Louie et al.*, 2005]. Nitrate enters liquid and/or solid phases through chloride depletion processes as follows [*Zhuang et al.*, 1999a, 1999b]:

$$\text{R1} \qquad HNO_{3(g)} + C1^- \leftrightarrow NO_3^- + HCl_{(g)}$$

[19] The observations at the HK University of Science and Technology (Latitude: 22.34 N; Longitude: 114.27 E) on 7 and 8 May 1998 are selected to set up a test case. The meteorological observations at several monitoring sites in the HK area during 7–8 May show that the atmosphere over HK was not stagnant but generally consistent in terms of wind speed/directions (which brought clean sea salt aerosols into this area) and solar irradiance [*Yao et al.*, 2001]. While similar meteorological conditions imply similar removal processes, similar solar irradiance would give similar chemical production rates for photochemically generated species such as H_2SO_4 and HNO_3, given the same initial amounts of reactants. Figure 3 shows the trajectories of marine air masses arriving HK every 4 h on 8 May 1998 (until 16 UTC 8 May 1998. i.e., 0000 9 May 1998 local time) simulated by HYSPLIT. As expected, the differences in the simulated trajectories arriving at HK on 8 May were very small, indicating similar air masses throughout 8 May. Our box model chemical kinetic simulation and analysis would be valid if (1) the air mass reaching HK on 7 May was stagnant until 8 May, or (2) the meteorological conditions over HK and the air masses passing HK on 7 and 8 May were similar and the changes in chemical concentrations were governed by the temporal evolution of the atmosphere rather than the spatial gradients in the modeling domain (i.e., the air parcel simulated in the box model had a homogeneous spatial distribution along its trajectory). The observations over HK and the trajectory analyses support the occurrence of the second scenario on 7–8 May 1998. Without anthropogenic emission sources for precursors of sulfate, nitrate and ammonium upwind, similar clean air masses from ocean will likely result in an approximately homogeneous spatial distribution for those secondary aerosols along the air mass trajectories. The observed aerosol concentrations at the HK site can be therefore assumed to be identical to the initial concentration upwind on the 24-h back-trajectory. Under such conditions, the temporal change in the aerosol concentrations observed over a 24-h interval at the HK site to be simulated with the box model can be assumed to represent the temporal change over 24 h in the concentrations simulated along the trajectory. Similar scenario has indeed been observed for the CRPAQS case over the California Central Valley (CCV) where the observed concentrations of $PM_{2.5}$, in particular, nitrate, show less spatial variability than temporal variability in winter, resulting in a homogeneous distribution over CCV [*Watson et al.*, 2005; *Chow et al.*, 2006a]. For the HK case, the assumption can be verified by comparing the box model simulation results after 24 h with the corresponding observations good agreement will support the assumption made here. Since no source/sink information was available on 7–8 May, certain assumptions must be made to characterize emission and removal processes. By carefully choosing data sets from the two days with consistent meteorological parameters and air masses, the perturbation to the chemical system of interest due to the variations in sources/sinks can be therefore minimized.

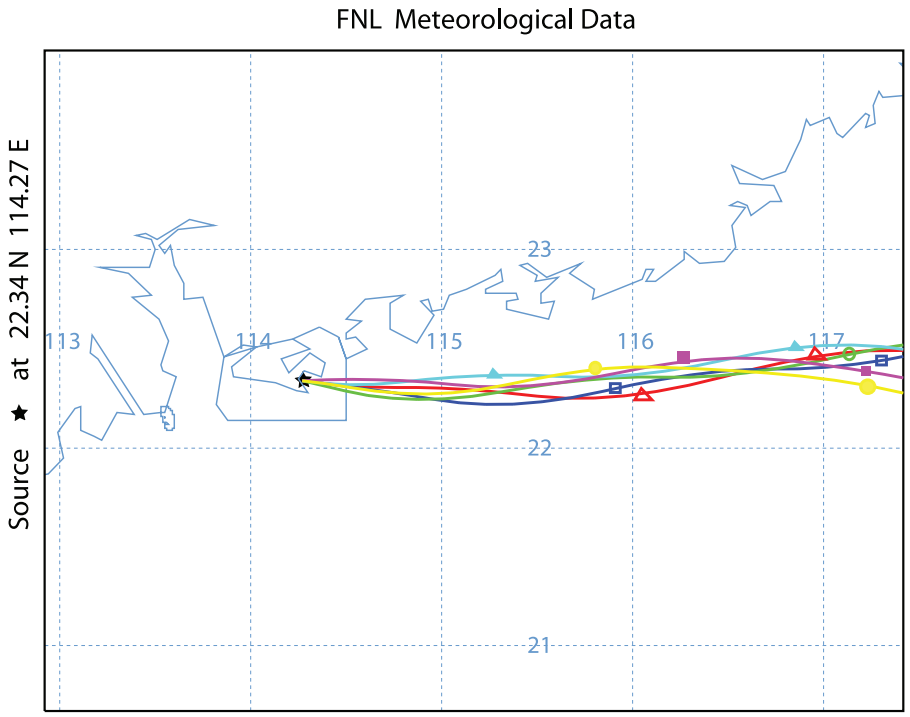

Figure 3. Trajectory of marine air masses arriving in Hong Kong every 4 h on 8 May 1998 simulated by HYSPLIT (http://www.arl.noaa.gov/ready/hysplit4.html). The line with hollow triangles, hollow squares, hollow circles, solid triangles, solid squares, and solid circles represent the air mass arriving in Hong Kong at 2400, 2000, 1600, 1200, 0800, and 0400 local time on 8 May respectively.

Under the consistent meteorological and homogeneous air mass conditions on 7–8 May, it is assumed that the differences in the observed aerosol mass on both days are caused by differences in emissions during the two days. Such a difference is considered as emissions to constrain the initial and final total compositions in our box model simulation.

[20] The measured species include nitric acid (HNO_3) and ammonia (NH_3) in the gas-phase and sulfate (SO_4^{2-}), nitrate (NO_3^-), chloride (Cl^-), ammonium (NH_4^+), sodium (Na^+), potassium (K^+), magnesium (Mg^{2+}), and calcium (Ca^{2+}) in the liquid and/or solid phases. Since K^+, Mg^{2+}, and Ca^{2+} are not treated in ISORROPIA, their measured concentrations are not used in the initial conditions for MADRID box model simulations. The total cation considered in MADRID is calculated as a sum of molar concentrations of NH_4^+ and Na^+. Since the observations of hydrochloric acid (HCl) are not available, a value of 0.1 ppb, typical of the marine boundary layer, is assumed [*Fridlind and Jacobson*, 2000]. *Fridlind and Jacobson* [2000] found that any estimation of HCl between 0.1–0.3 ppb (or 0.15–0.46 $\mu g\ m^{-3}$) may not exceed the experimental uncertainty in Cl^- measurements and would not significantly affect the partitioning of chloride. The measured aerosol size/composition distributions (see Figure 4a) by Micro-Orifice Uniform Deposit Impactor (MOUDI) on 7 May 1998 are used as inputs for MADRID to simulate the formation of aerosols for a 24-h period (i.e., May 8). Since the MOUDI is size-segregated, the sampling artifact due to interparticle interactions [*Pathak et al.*, 2004] is relatively small [*Yao et al.*, 2001]. The meteorological variables on 8 May 1998 (i.e., temperature (T) of 302.15 K and relative humidity (RH) of 86%) are used in the MADRID box model simulations. Sulfate and nitrate are mostly formed from H_2SO_4 and HNO_3. Since differences in meteorology and air masses reaching HK on the two consecutive days (7 and 8 May) are small, we assume that differences in the total mass of sulfate, nitrate, chloride, and ammonium on the two days are due to differences in emissions of gas precursor species of $PM_{2.5}$. Differences in total mass (summed over both the aerosol and gas phases) of each species on 8 May 1998 and those on 7 May 1998 are therefore treated as emissions (i.e., source) for 8 May to constrain the initial and final total compositions in our box model simulation. They (except Na^+) are added to the concentrations of the corresponding gas-phase species. The resultant gas phase concentration used by the box model is 0.309 ppb HNO_3; 0.198 ppb H_2SO_4; 1.76 ppb NH_3; and 0.31 ppb HCl on 7 May. Difference in the Na^+ concentrations between the two days is injected into the liquid and/or solid phases. Table 2a shows the initial ratios of molar concentrations of cations (R_{cation}) and sodium (R_{Na}) to the molar concentration of total sulfate for each aerosol section, where [*Nenes et al.*, 1998]:

$$R_{cation} = \frac{[Na^+] + [NH_4^+]}{[SO_4^{2-}]},$$

$$R_{Na} = \frac{[Na^+]}{[SO_4^{2-}]} \tag{2}$$

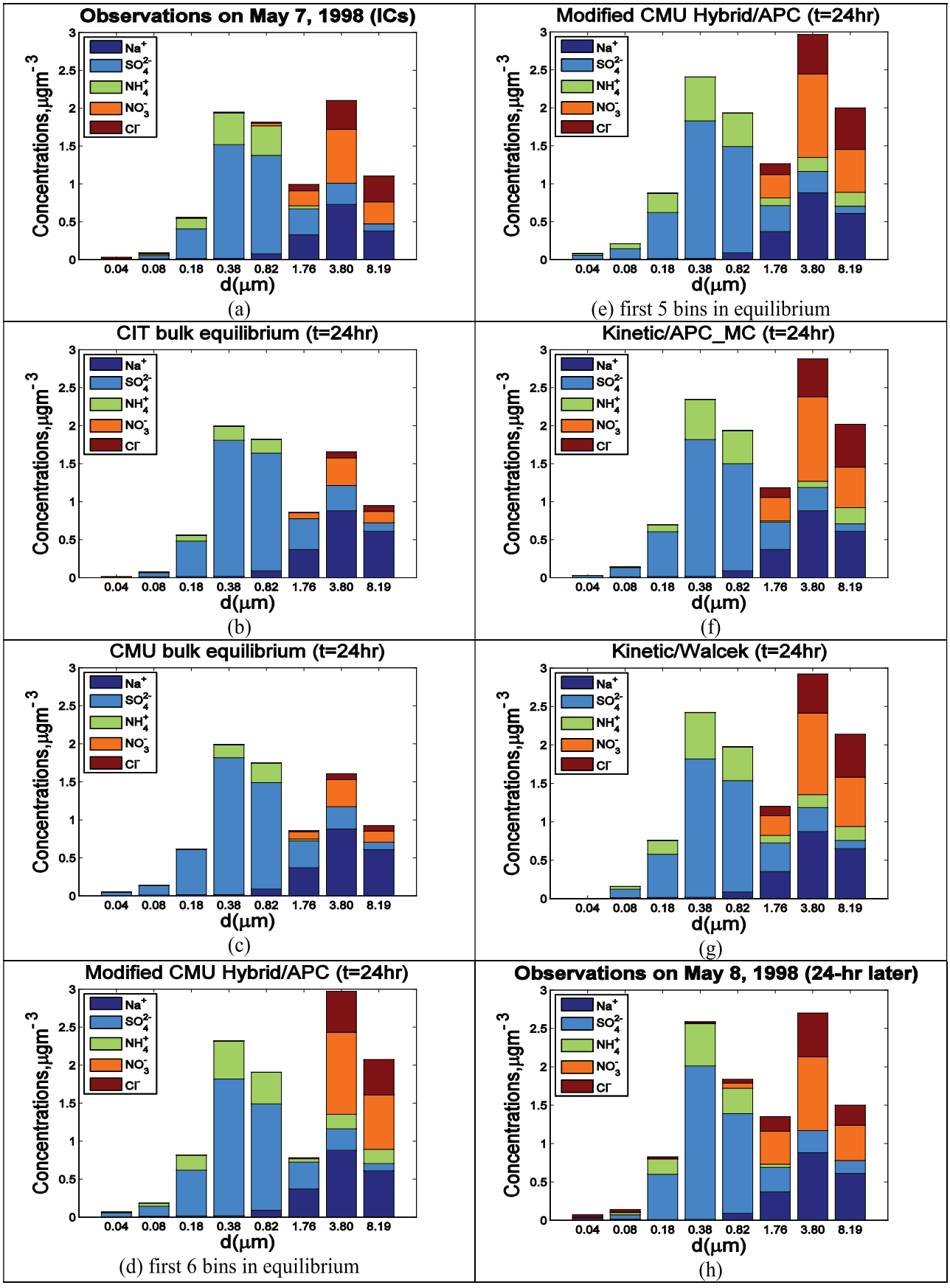
Observations on May 7, 1998 (ICs)
Modified CMU Hybrid/APC (t=24hr)
CIT bulk equilibrium (t=24hr)
Kinetic/APC_MC (t=24hr)
CMU bulk equilibrium (t=24hr)
Kinetic/Walcek (t=24hr)
Modified CMU Hybrid/APC (t=24hr)
Observations on May 8, 1998 (24-hr later)
Concentrations,μgm-3
d(μm)
0.04 0.08 0.18 0.38 0.82 1.76 3.80 8.19
Na+
SO4 2-
NH4+
NO3-
Cl-
(a)
(e) first 5 bins in equilibrium
(b)
(f)
(c)
(g)
(d) first 6 bins in equilibrium
(h)

Figure 4

Table 2. Measured Size-Resolved Aerosol Chemical Regimes

	Bin 1	Bin 2	Bin 3	Bin 4	Bin 5	Bin 6	Bin 7	Bin 8
				(a) Hong Kong on 7 May 1998				
R_{cation}	N/A[a]	3.7	2.1	1.6	1.9	4.8	11.1	16.9
R_{Na}	N/A[a]	1.2	0.2	0.1	0.3	4.2	11.1	16.9
Chemical regime[b]	S-poor Na-rich	S-poor Na-poor	S-poor Na-poor	S-rich Na-poor	S-rich Na-poor	S-poor Na-rich	S-poor Na-rich	S-poor Na-rich
Cation/anion[c]	0.33	1.26	1.02	0.78	0.94	1.34	1.14	1.00
				(b) Tampa Bay, FL on 3–9 May 2001				
R_{cation}	1.8	1.9	2.0	2.1	2.0	2.2	4.8	6.4
R_{Na}	0.1	0.1	0.1	0.0	0.1	2.0	4.6	6.2
Chemical regime[b]	S-rich Na-poor	S-rich Na-poor	S-poor Na-poor	S-poor Na-poor	S-poor Na-poor	S-poor Na-rich	S-poor Na-rich	S-poor Na-rich
Cation/anion[c]	0.89	0.95	1.00	0.94	0.98	0.71	0.62	0.61
				(c) Angiola, CA on 17 December 2000				
R_{cation}	N/A	27.1	6.5	8.1	4.6	4.1	N/A	N/A
R_{Na}	N/A	19.0	0.3	0.2	1.9	2.7	N/A	N/A
Chemical regime[b]	S-poor Na-rich	S-poor Na-rich	S-poor Na-poor	S-poor Na-poor	S-poor Na-poor	S-poor Na-rich	S-poor Na-rich	S-poor Na-rich
Cation/anion[c]	N/A	9.73	1.20	1.17	1.78	1.07	N/A	N/A

[a]N/A indicates that the ratio is not available because of zero concentrations of SO_4^{2-}.

[b]S-poor ($R_{cation} \geq 2$), S-rich ($R_{cation} < 2$), Na-poor ($R_{Na} < 2$), Na-rich ($R_{Na} \geq 2$) denote sulfate-poor, sulfate-rich, sodium-poor, and sodium-rich, respectively.

[c]NH_4^+, Na^+, SO_4^{2-}, NO_3^-, and Cl^- are counted when calculating the molar ratios of cation/anion. [SO_4^{2-}] is multiplied by 2 to account for the two negative charges. Observed H^+ concentrations are not available.

[21] In these equations, [Na^+], [NH_4^+], and [SO_4^{2-}] denote the molar concentrations of Na^+, NH_4^+, and SO_4^{2-}, respectively. Two different sources of aerosols can be seen in the sample on May 7. First, sodium, the tracer of sea-salt, is abundant in the three supermicrometer sections (sections 6–8). Second, sulfate is abundant in the accumulation mode (sections 4 and 5), indicating an anthropogenic source from the polluted urban area. The concentration ratios (in charge equivalents) between measured cations and anions are also shown in Table 2a. The cation-to-anion ratios in the accumulation mode are less than unity, indicating that this size range is acidic [*Kerminen et al.*, 2001; *Moya et al.*, 2003].

[22] Initial aerosol conditions and predictions from the equilibrium, kinetic, and hybrid approaches with 8 sections and those from benchmark (i.e., the kinetic/APC_MC, kinetic/Walcek approaches with 500 sections and a short time step of 0.5 s) at the HK site on 8 May 1998 are shown in Figures 4 and 5, respectively. The simulated aerosol composition with 500 sections is also aggregated into 8 sections in (b) and (c) to allow a direct comparison with corresponding 8-section results in Figures 4f–4g and observations in Figure 4h. For 8-section simulations, a time step of 15 s is used for the kinetic/APC_MC scheme according to *Jacobson* [1997b]. A time step of 0.5 s is used for the kinetic/Walcek scheme as the Walcek scheme is subjected to the Courant number limitation and requires a small time step [*Hu et al.*, 2005]. The box model is run for a 24-h period. The size-resolved distributions simulated by the kinetic approaches (with the APC_MC scheme (Figure 4f) and the Walcek scheme (Figure 4g)) at t = 24-h agree well with the measured distribution on 8 May 1998 (Figure 4h), with small differences in the ammonium distribution. The predictions from the CIT and CMU bulk equilibrium approaches (see Figures 4b and 4c), however, lost some NH_4^+ in the submicrometer sections and some NO_3^- and Cl^- in the supermicrometer sections to the gas phase. Their corresponding gas phase species (i.e., NH_3, HNO_3, and HCl) increase by 0.52, 0.68, and 0.70 $\mu g\ m^{-3}$, respectively as shown in Figure 6. This is due to the disadvantage of the equilibrium and internal mixture assumption associated with the bulk equilibrium approach. The equilibrium assumption may not work in this case since the aerosol state on 8 May 1998 may deviate from equilibrium as indicated by *Yao et al.* [2006, 2007]. Also NH_4^+ in the submicrometer sections and NO_3^- and Cl^- in the supermicrometer sections are treated together in the bulk phase, allowing the formation of ammonium nitrate (NH_4NO_3) and ammonium chloride (NH_4Cl). Since NH_4NO_3 and NH_4Cl are highly volatile (especially under the high temperature, 302.15 K, tested here), some of them evaporate. On the other hand, the kinetic approach uses a size-resolved treatment, allowing a separation of the fine mode NH_4^+ and the coarse mode NO_3^- and Cl^-. In such cases, coarse mode NO_3^- and Cl^- are associated with Na^+, which is nonvolatile, while fine mode NH_4^+ is associated with SO_4^{2-}, which is also nonvolatile [*Ackermann et al.*, 1998; *Baek et al.*, 2004; *Metzger et al.*, 2002]. The concurrent loss of NH_4^+ with NO_3^- and Cl^- therefore does not occur for the kinetic approaches. The prediction from the modified CMU hybrid/APC_MC approach for the last 2 sections is close to the prediction from the kinetic approach since they are also solved explicitly, except with slightly higher total mass concentration. The NO_3^- and Cl^- concentrations in section 5 predicted by the modified CMU hybrid/APC_MC approach with a threshold diameter of 2.15 μm are lost to the gas-

Figure 4. Initial size-resolved aerosol composition on 7 May 1998 and simulated composition on 8 May 1998 by the equilibrium, kinetic, and hybrid approaches in box MADRID at the Hong Kong site. The measured size-resolved aerosol composition on 8 May is also shown in Figure 4h.

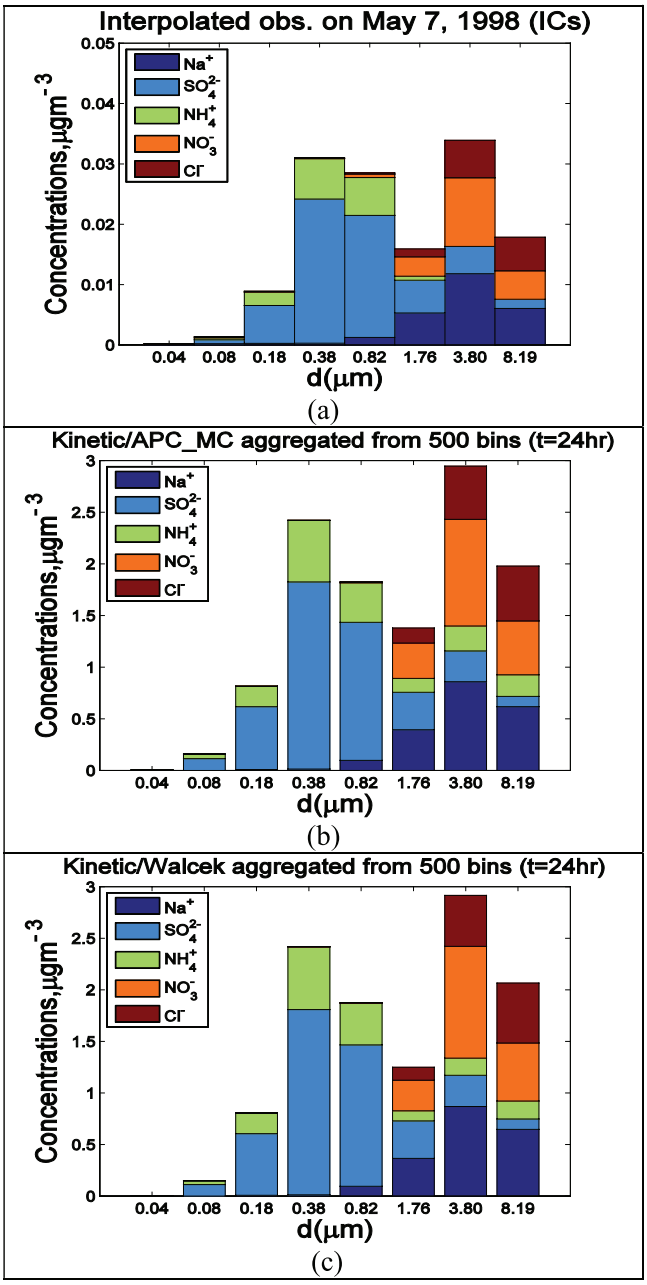

Figure 5. Initial size-resolved aerosol composition with 500 size sections on 7 May 1998 and simulated composition on 8 May 1998 by kinetic/APC_MC and kinetic/Walcek at the Hong Kong site. The simulated aerosol composition with 500 sections is aggregated into 8 sections in Figures 5b and 5c for a direct comparison with Figures 4f–4h.

phase (Figure 4d), however, because of the aforementioned disadvantage of the bulk equilibrium treatment. Since the value of this threshold diameter affects its performance, a sensitivity simulation is conducted using a lower threshold diameter of 1.0 μm (i.e., gas/particle mass transfer for sections 6–8 is solved explicitly while treating the first 5 sections with an equilibrium approach). When the threshold diameter is reduced from 2.15 to 1.0 μm, the modified CMU hybrid/APC_MC approach gives closer agreement to the observed size-resolved composition on 8 May 1998, because section 6 is not in the equilibrium state and its prediction can be improved with the kinetic approach. Total nitrate over all bins predicted with a threshold diameter of 1.0 μm is higher than that predicted with a threshold diameter of 2.15 μm (1.97 versus 1.81 μg m^{-3}).

[23] Among all approaches tested, the kinetic/APC_MC and kinetic/Walcek give overall best agreement with the observations in terms of both size-resolved aerosol distribution and the gas-phase concentrations of HNO_3 and NH_3 as shown in Figures 4 and 6. Comparing with the predictions from benchmarks, modified CMU hybrid/APC_MC, kinetic/APC_MC, and kinetic/Walcek all give closer prediction than the bulk equilibrium approaches. The performance statistics for five individual PM species and their total mass against observations and the two benchmarks with kinetic approaches are shown in Table 3a. In terms of size-resolved aerosol distribution, kinetic/APC_MC and kinetic/Walcek predict the most accurate distributions. Comparing with the observed distribution on 8 May 1998 (Figure 4h), the NMEs of total mass are 28.0%, 27.9%, 16.4%, 12.5%, and 13.3% for the CIT equilibrium, the CMU equilibrium, the modified CMU hybrid/APC_MC, the kinetic/APC_MC, and the kinetic/Walcek approaches, respectively. Overall the kinetic/APC_MC and kinetic/Walcek approaches give lower errors for volatile species (i.e., NH_4^+, NO_3^-, and Cl^-) and similar statistics for nonvolatile species such as Na^+ and SO_4^{2-}.

[24] A comparison of 8-section simulation results in Figure 4 to the benchmarks in Figure 5 also shows that simulated size-resolved aerosol composition with the 8-section modified CMU hybrid, the kinetic/APC_MC and the kinetic/Walcek approaches are more accurate than the full equilibrium approaches. These approaches predict NH_4^+ in the fine mode and Cl^- and NO_3^- in coarse mode, which is consistent with the benchmarks. The NMEs are 8.6%, 5.7% and 4.9%, respectively, for the total PM mass from the 8-section modified CMU hybrid, the kinetic/APC_MC and the kinetic/Walcek approaches against the predicted distribution from the 500-section kinetic/APC_MC benchmark (Figure 5b), whereas the NMEs for bulk equilibrium approaches can be as high as 32%. While the overall mass distribution predicted by the 8-section kinetic/APC_MC with 15-s time step is fairly close to that predicted by benchmark with the 500-section kinetic/APC_MC approach, small differences exist for volatile species such as NH_4^+, due to the sensitivity of this approach to time step and size resolution used for testing.

[25] The observed distribution on 8 May 1998 shown in Figure 4(h) is in good agreement with the benchmarks shown in Figure 5(b) and 5(c) (except some differences for volatile species in the coarse mode (e.g., NH_4^+), which may be due to the evaporation of volatile species from the MOUDI measurement without denuders [*Yao et al.*, 2001]). This agreement further verifies that the assumption made for the box model simulation appears to be reasonable.

[26] Figure 7 shows the predicted hourly concentrations of volatile species (i.e., NO_3^-, Cl^-, and NH_4^+) from the two kinetic approaches with 8 and 500 sections. Note that the two kinetic approaches with 8 sections are tested with a number of time steps (0.25–0.5 s for kinetic/Walcek and 0.25–30 s for kinetic/APC_MC), the results shown in

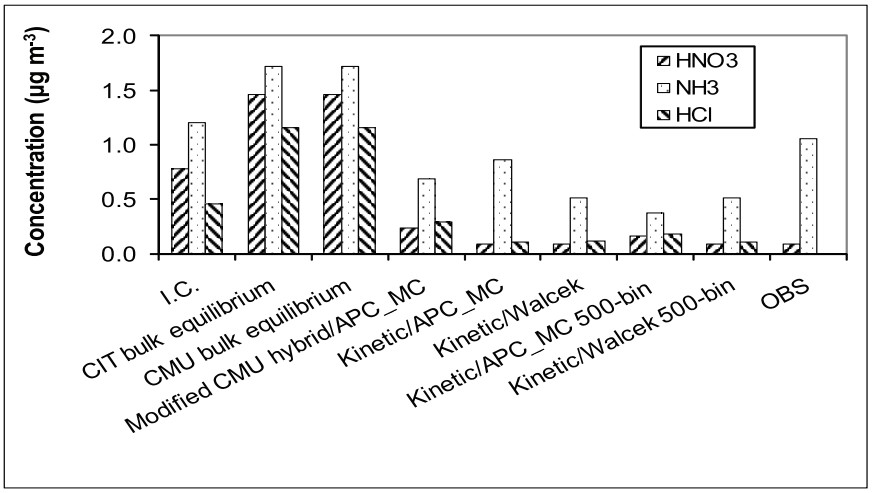

Figure 6. Initial gas-phase concentrations of three volatile species (i.e., HNO_3, NH_3, and HCl) and those at t = 24 h predicted by the equilibrium, kinetic, and hybrid approaches in box MADRID at the Hong Kong site. The observed concentrations of HNO_3 and NH_3 are also plotted. No observations are available for HCl. The threshold for the modified CMU hybrid/APC_MC approach is 2.15 μm.

Figure 7 are obtained with a time step of 15 s for kinetic/APC_MC and 0.5 s for kinetic/Walcek, corresponding to those shown in Figures 4f and 4g. As shown in Figure 7, the two kinetic approaches with 500 sections and 0.5 s give overall similar results. Their results with 8 sections and the same time step (e.g., 0.25–0.5 s) are also very similar (Figures for kinetic/APC_MC with short time steps are not shown). The differences in the time evolution of NH_4^+, NO_3^-, and Cl^- in each section with 8-section between the two kinetic approaches are caused primarily by the use of different time steps. Appreciable oscillation may occur at a long time step (typically > 15 s) for any growth scheme coupled with any equilibrium scheme due to delays in feedbacks between the equilibrium and growth calculations when the operator-splitting method is used [*Jacobson*, 2005]. However, the oscillation and its effect are much smaller at a high relative humidity than at a low RH. Our test results with observational data are consistent with *Jacobson* [2005]. As the time step reduces from 30 s to 0.25 s, the simulated time evolution of species with 8 sections becomes closer to that predicted with 500 sections and 0.25 s. While kinetic/Walcek requires a small time step (e.g., 0.5 s) to produce accurate results, kinetic/APC with 8 sections gives results that are reasonably close to the observed size distribution given a coarse size resolution of 8-section and a long time step of 15 s (see Figure 4).

[27] The evaporation of volatile species depends highly on T and RH. To examine this sensitivity, the bulk equilibrium approach is applied to the same HK test case but with different T and RH conditions. The results are shown in Figure 8. With a fixed RH of 86%, the predicted concentrations of NO_3^-, NH_4^+, and Cl^- in the liquid and/or solid phases concurrently increase and approach the observations at HK on 8 May 1998 as T decreases from 302.15 K to 293 K (Figure 8a). A similar trend is shown in Figure 8b as RH increases from 86% to 96%. Decreasing T and increasing RH suppress the concurrent losses of NO_3^-, NH_4^+, and Cl^-. The concurrent evaporation of volatile species (i.e., NO_3^-, NH_4^+, and Cl^-) from the liquid and/or solid phases under the relatively high T and low RH conditions on May 8 in the bulk equilibrium treatments can therefore be explained by the above sensitivity experiment. As shown in Figures 8a and 8b, the bulk equilibrium approach predicts more NO_3^- and less Cl^- than observations at low T (e.g., 293 K) and high RH (e.g., 96%).

[28] Tampa Bay (TB), FL, U.S. is an estuary and coastal area, which is affected by several local industrial and utility sources of nitrogen oxide, sulfur dioxide and ammonia [*Poor et al.*, 2001] and sea salt emissions. The aerosol loading in TB (especially nitrogen loading) attracts some research interests because of its eutrophication effects [*Poor et al.*, 2001; *Evans et al.*, 2004]. Accurately predicting mass transfer process is critical for predicting species concentrations since the deposition velocity depends on the phase state and aerosol size if the species is residing in the liquid and/or solid phases [*Russell et al.*, 1993]. A 6-d cumulative aerosol measurement using cascade impactor and concurrent gas-phase measurements during 3–9 May 2001 in TB [*Campbell et al.*, 2002] are used to set up the test case. The observed aerosol distributions that are used as inputs for the model are shown in Figure 9a. The chemical regimes for each section are provided in Table 2b. The cation-to-anion ratios in the last two sections are significantly low, which may be due partially to the exclusion of Ca^{2+} and other species in the original measurements [*Campbell et al.*, 2002]. The back trajectories of air arriving in TB during 3–9 May 2001 (Figure not shown here), suggest dominant marine sources and possible terrestrial origins of the aerosols and similar air mass composition during the simulation period. The 6-d average T (297.05 K) and RH (62.2%) are used in the test case for a 48-h simulation to allow sufficient time to reach equilibrium. The aerosol concentrations of NO_3^-, NH_4^+, Cl^-, SO_4^{2-}, and Na^+ in TB shown in Figure 9a are similar to those in HK. It is, however, sulfate-poor in the accumulation mode and sulfate-rich in the nuclei mode, which are opposite to those in the above HK case. The different T and RH conditions in TB may affect the phase state of some salts (e.g., whether solid or aqueous). For

Table 3. Normalized Mean Error (NME) of Predicted Distributions From 8-Bin Kinetic/APC_MC and Kinetic/Walcek Against Observed (Except for Tampa Bay) and Those From 500-Bin Kinetic/APC_MC and Kinetic/Walcek

	CIT Bulk Equilibrium			CMU Bulk Equilibrium			Modified CMU Hybrid/APC_MC			Kinetic/APC_MC			Kinetic/Walcek		
Benchmark	Obs.	500-bin kinetic/ APC_MC	500-bin kinetic/ Walcek	Obs.	500-bin kinetic/ APC_MC	500-bin kinetic/ Walcek	Obs.	500-bin kinetic/ APC_MC	500-bin kinetic/ Walcek	Obs.	500-bin kinetic/ APC_MC	500-bin kinetic/ Walcek	Obs.	500-bin kinetic/ APC_MC	500-bin kinetic/ Walcek
(a) Hong Kong on 7 May 1998															
Na^+	2.2%	4.4%	4.4%	2.2%	4.4%	4.4%	2.2%	4.4%	4.4%	2.2%	4.4%	4.4%	5.9%	6.1%	2.7%
SO_4^{2-}	16.4%	11.6%	10.0%	11.5%	3.5%	2.7%	11.8%	3.8%	3.1%	11.3%	3.1%	2.0%	12.1%	4.6%	3.1%
NH_4^+	60.4%	74.8%	73.1%	60.4%	74.8%	73.0%	47.3%	16.8%	13.2%	50.1%	29.9%	26.6%	51.4%	12.5%	3.9%
NO_3^-	69.4%	69.2%	69.9%	69.4%	68.5%	69.2%	46.4%	30.8%	23.0%	23.0%	6.8%	3.6%	28.6%	12.5%	7.3%
Cl^-	86.0%	87.1%	87.2%	86.0%	86.5%	86.5%	48.5%	19.3%	23.5%	49.6%	5.9%	2.2%	48.9%	5.2%	3.4%
Total	28.0%	31.4%	31.2%	27.9%	32.0%	31.8%	16.4%	8.6%	6.7%	12.5%	5.7%	3.7%	13.3%	4.9%	2.5%
(b) Tampa Bay, FL on 3–9 May 2001															
Na^+	N/A	1.7%	1.7%	N/A	1.7%	1.7%	N/A	1.7%	1.7%	N/A	1.7%	1.7%	N/A	1.7%	1.7%
SO_4^{2-}	N/A	2.4%	2.4%	N/A	2.4%	2.4%	N/A	2.4%	2.4%	N/A	2.4%	2.4%	N/A	2.4%	2.4%
NH_4^+	N/A	43.7%	44.6%	N/A	37.9%	47.4%	N/A	19.3%	2.7%	N/A	17.6%	25.5%	N/A	20.3%	3.4%
NO_3^-	N/A	100.0%	100.0%	N/A	100.0%	100.0%	N/A	20.7%	5.3%	N/A	23.1%	13.4%	N/A	38.8%	16.3%
Cl^-	N/A	100.0%	100.0%	N/A	100.0%	100.0%	N/A	41.5%	25.3%	N/A	60.8%	85.0%	N/A	100.0%	100.0%
Total	N/A	23.4%	24.9%	N/A	23.4%	24.9%	N/A	3.1%	1.5%	N/A	5.0%	3.9%	N/A	4.8%	3.0%
(c) Angiola, CA on 17 Dec 2000															
Na^+	0.0%	54.8%	47.5%	0.0%	54.8%	47.5%	0.0%	54.8%	47.5%	0.0%	54.8%	47.5%	2.4%	53.2%	47.3%
SO_4^{2-}	15.9%	6.9%	6.1%	20.1%	6.3%	8.2%	20.1%	6.3%	8.2%	21.1%	5.8%	7.8%	19.3%	5.2%	5.4%
NH_4^+	9.1%	19.6%	15.3%	19.0%	10.7%	7.7%	18.6%	8.8%	5.8%	21.6%	7.7%	7.2%	20.3%	7.7%	8.0%
NO_3^-	24.4%	25.8%	22.3%	35.8%	12.0%	9.9%	35.8%	12.0%	9.9%	35.4%	10.2%	8.1%	31.8%	10.5%	7.5%
Cl^-	14.1%	37.3%	31.5%	39.1%	13.1%	9.6%	39.1%	13.1%	9.6%	32.8%	11.8%	7.6%	48.0%	19.2%	20.2%
Total	17.2%	23.1%	19.3%	26.8%	9.1%	8.0%	27.3%	9.5%	8.4%	27.2%	8.5%	7.4%	25.2%	9.2%	7.8%

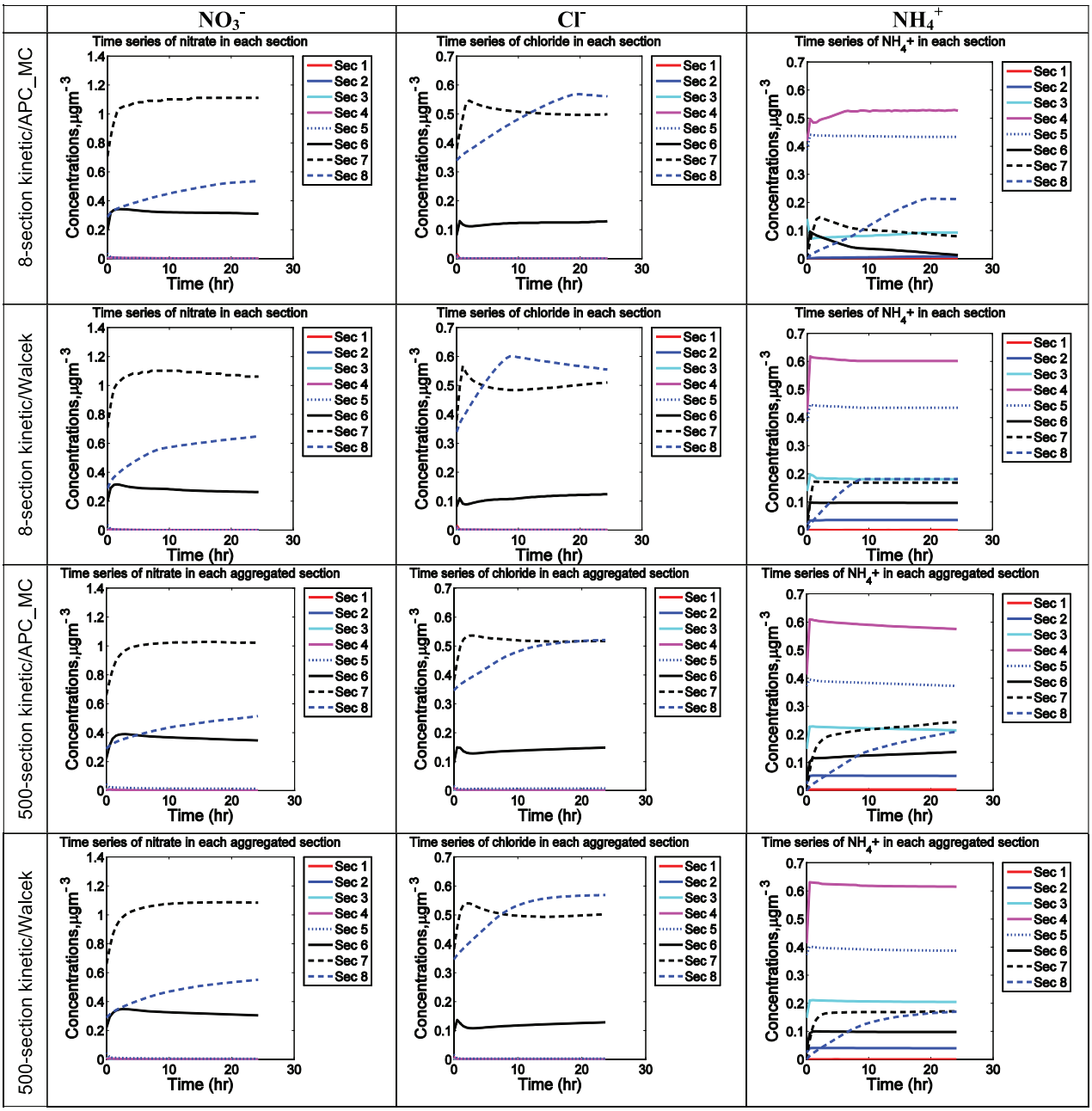

Figure 7. Predicted time series of volatile species (i.e., NO_3^-, Cl^-, and NH_4^+) with 8-section kinetic/APC_MC, kinetic/Walcek and 500-section kinetic/APC_MC, kinetic/Walcek. The 8-section results are obtained with a time step of 15 s for kinetic/APC_MC and 0.5 s for kinetic/Walcek. The results from the 500-section kinetic approaches are aggregated into 8 sections.

example, NH_4Cl may stay in the solid phase since its deliquescence relative humidity (DRH) is 80% at 298 K [*Seinfeld and Pandis*, 1998]. The results from the three gas/particle mass transfer approaches are shown in Figure 9. No observations are available after a 48-h period for model evaluation. Simulation results with 8 sections are evaluated against the two benchmarks shown as aggregated 8-section distributions in Figures 9g and 9h. Similar to the HK test case on 7–8 May 1998, the concurrent loss of submicrometer NH_4^+ and supermicrometer Cl^- and NO_3^- occur for the bulk equilibrium predictions, for the same reasons as stated previously. The fact that the sampled aerosol may not be in equilibrium [*Campbell et al.*, 2002] also explains the deviation of the bulk equilibrium predictions from the initial condition. Comparing with the benchmarks with 500 sections, the modified CMU hybrid/APC_MC, kinetic/APC_MC and kinetic/Walcek approaches with 8 sections predict similar distributions for all size bins. As shown in Table 3b, their NMEs are much smaller than those for CIT and CMU bulk equilibrium approaches, particularly for volatile species.

[29] Compared with the initial distribution, all the three approaches predict more nitrates and significantly less chloride in the coarse mode (i.e., sections 7 and 8). The

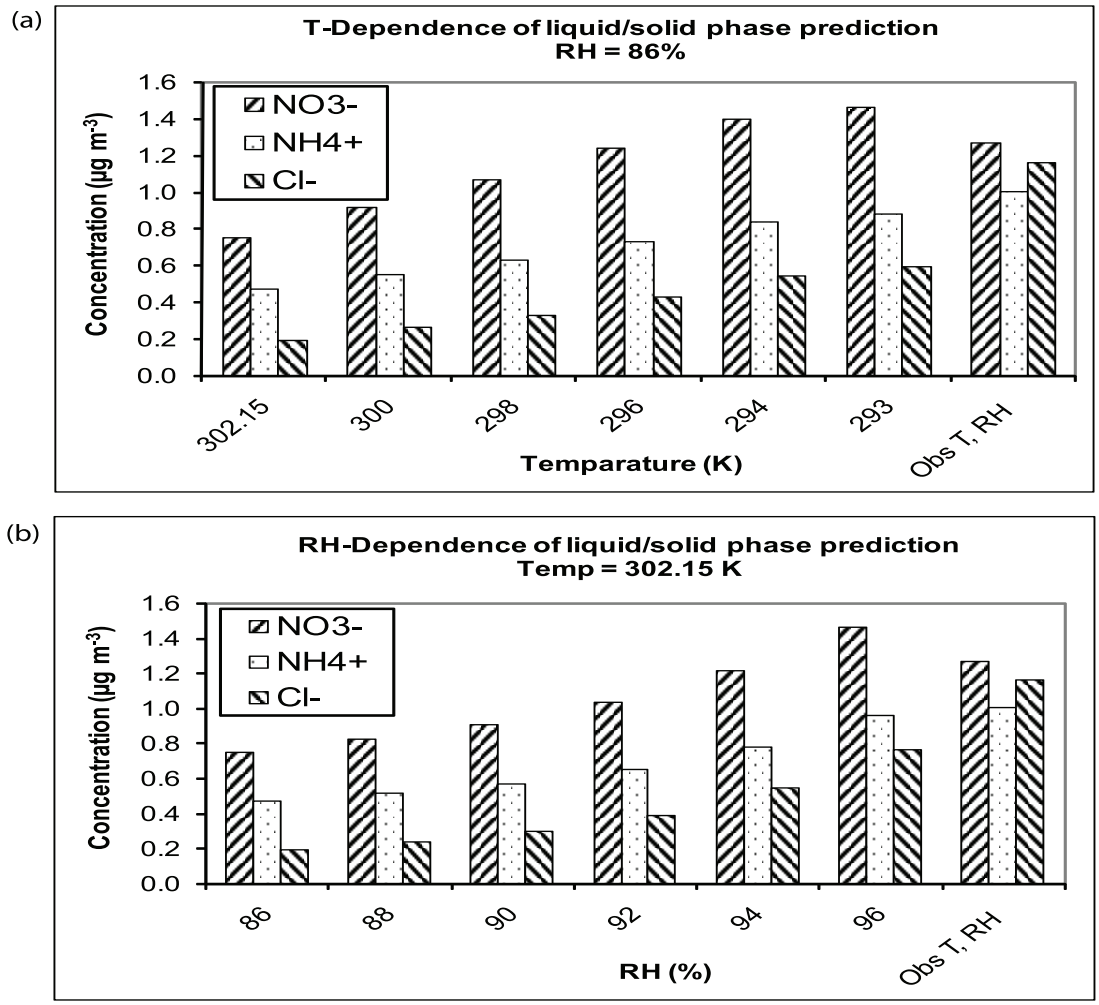

Figure 8. T- and RH-dependence of liquid/solid phase predictions by the CIT bulk equilibrium approach. The observed T and RH are 302.15 K and 86%, respectively.

significant deviation from the initial distribution in resulting chloride size distribution may indicate a need for treating crustal species in ISORROPIA under the conditions with an initial cation/anion ratio of less than 1 (see Table 2). Given initially insufficient cations but excessive anions when only Na^+ and NH_4^+ are considered as cations, nearly all Cl^- are forced to evaporate to the gas-phase as HCl (see Figure 9), illustrating a need to treat crustal species (e.g., K^+, Mg^{2+}, and Ca^{2+}) to avoid the departure of Cl^- from the particulate phase under such conditions. This is consistent with the finding of *Ansari and Pandis* [1999] that a lack of treatment for crustal species in aerosol thermodynamic modules may give low anion predictions. Separate simulations with the EQUISOLV II thermodynamic module with and without treating crustal species for the same TB case also verify that treating crustal species can form more salts of Cl^- (e.g., KCl, $MgCl_2$, and $CaCl_2$) in the coarse sections (Figures not shown). For comparison, when the initial cation/anion ratios are sufficiently high (e.g., > 1 for the HK case, see Table 2), the lack of treatment for crustal species has a much smaller effect on the overall model predictions which are reasonably close to the observations (see Figure 4). The departure from the initial distribution for the TB case also indicates that the coarse mode may not be in equilibrium with the gas phase, which is consistent with the findings of *Campbell et al.* [2002]. When the threshold diameter is reduced from 2.15 to 1.0 μm (Figure not shown), the modified CMU hybrid/APC_MC approach does not show closer agreement to the initial distribution, because section 6 is already in the equilibrium state and its prediction with an equilibrium approach is very similar to that with the kinetic approach.

[30] PM concentration exceedances over the National Ambient Air Quality Standards in the California San Joaquin Valley (SJV) are frequent especially during fall and winter [*Pun and Seigneur*, 1999] owing to the combination of mobile, industrial, agricultural, and residential sources [*McDade*, 2002]. Secondary NH_4NO_3 is the largest contributor of PM concentration during winter across the SJV region for both urban and rural areas [*Magliano et al.*, 1999]. CRPAQS is a multiyear observational and modeling study that involved multiple organizations and was conducted in northern California with a focus on the Central Valley. Since nitrate in the SJV showed a rather uniform spatial variability [*Watson et al.*, 2005; *Chow et al.*, 2006a], the observations in Angiola on 17 and 18 December 2000 from the CRPAQS are used to set up the third box model

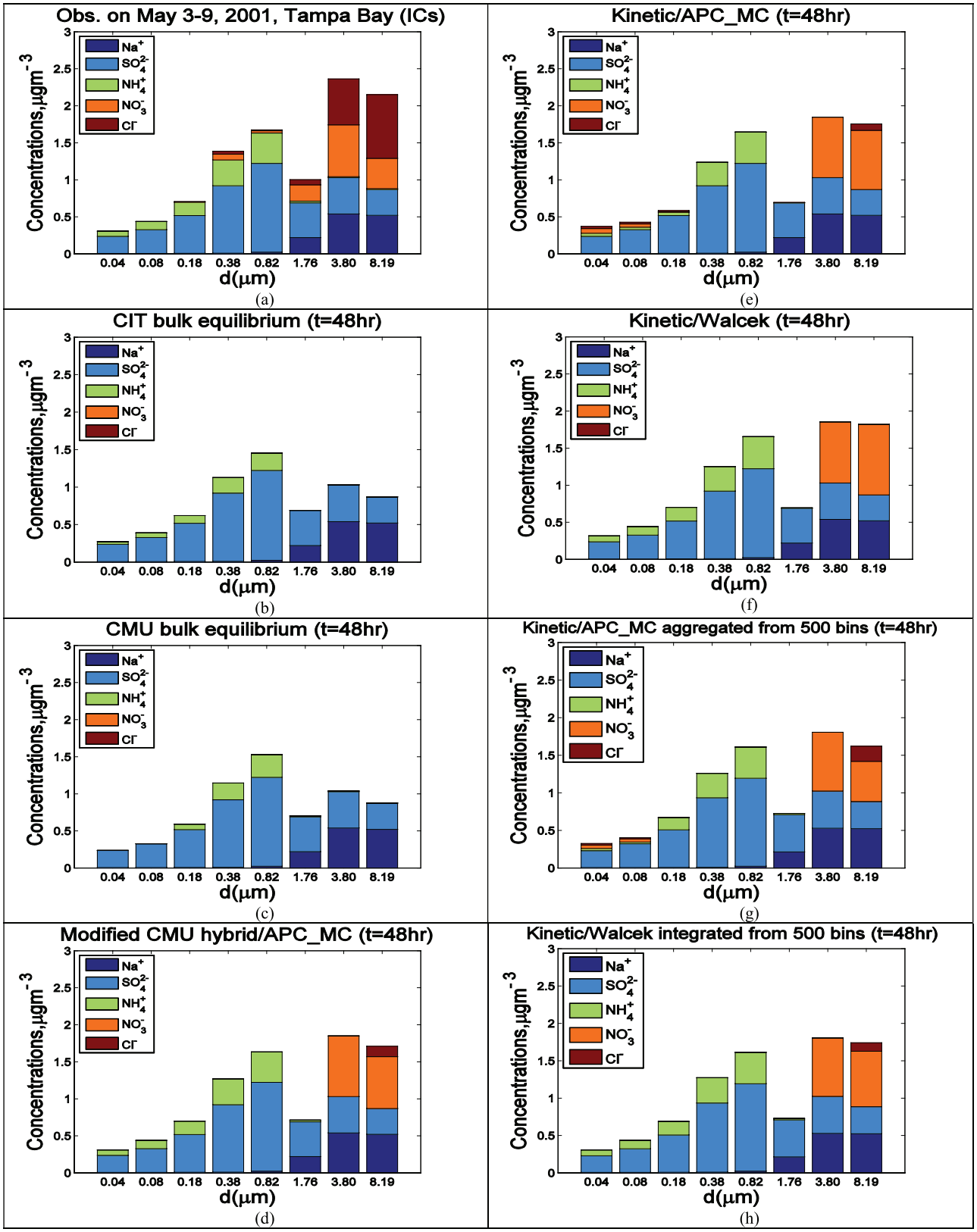

Figure 9. Initial size-resolved aerosol composition on 3–9 May 2001 and simulated composition 48 h later by the bulk equilibrium, hybrid, and kinetic approaches in box MADRID with 8 sections ((a)–(f)) and that by the kinetic approaches with 500 sections ((g) and (h)) in Tampa Bay. No observed aerosol concentrations are available for comparison. The results from the 500-section kinetic approaches are aggregated into 8 sections.

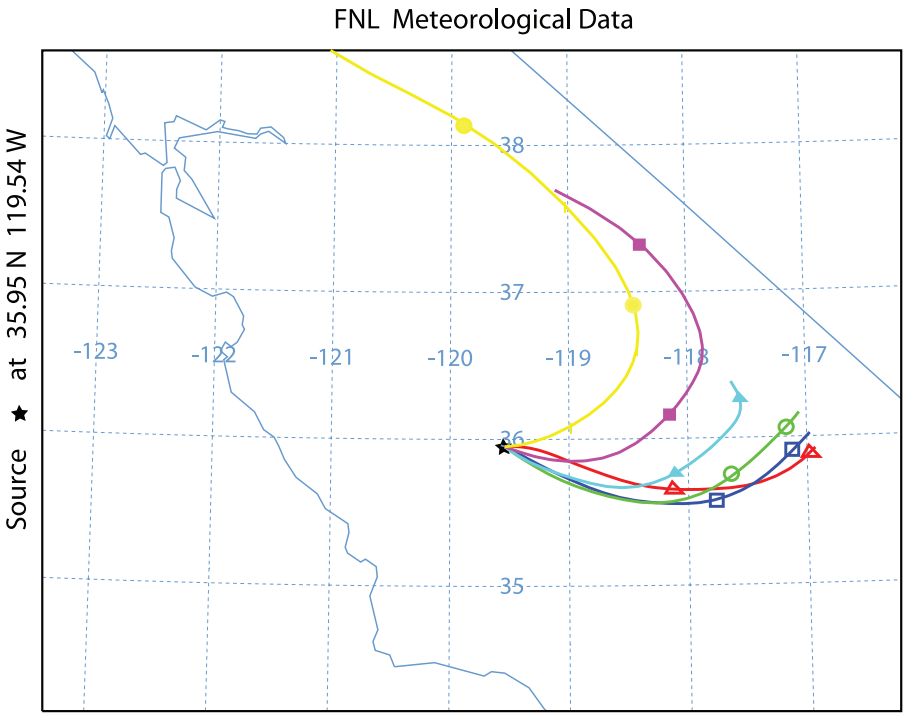

Figure 10. The trajectory of air masses arriving in Angiola every 4 h on 18 December 2000 simulated by HYSPLIT (http://www.arl.noaa.gov/ready/hysplit4.html). The line with hollow triangles, hollow squares, hollow circles, solid triangles, solid squares, and solid circles represent the air mass arriving Angiola at 2400, 2000, 1600, 1200, 0800, and 0400 local time on 18 December, respectively.

test case (referred to as the CRPAQS/AN case) using the same approach as the HK case. The back trajectories of air masses arriving at Angiola every 4 h on 18 December 2000 are shown in Figure 10, which indicates the regional sources in Angiola on Dec. 18. While air trajectories in the morning were different, they converged during the rest of day. The measured aerosol size composition on 17 December is used as inputs into MADRID (see Figure 11a). This case represents sulfate-poor conditions; it differs significantly from the previous two cases with negligible aerosol mass in the coarse mode. The difference of total mass on 17 and 18 December is considered as an additional source in the gas phase for SO_4^{2-}, NH_4^+, NO_3^-, and Cl^- and in the liquid and/or solid phases for Na^+. For this case, NH_4^+ and NO_3^- dominate the accumulation mode, indicating a sulfate-very poor (or ammonia-very rich) and nitrate-rich condition at Angiola during this study [*Wang et al.*, 2006]. The meteorological variables on 18 December (i.e., T of 278.13 K and RH of 98.6%) are used in the box model simulation. Initial size-resolved aerosol composition on 17 December 2000 and simulated size resolved composition on 18 December 2000 are shown in Figure 11. In addition to observed aerosol size distribution on 18 December (Figure 11i), simulation results are evaluated against the benchmarks shown as the aggregated 8-section distributions in Figures 11g and 11h. The distributions predicted by all 8-section simulations are very close to the benchmarks and the observations. The statistics for each approach shown in Table 3c are comparable for this test case. The differences in the size-resolved aerosol composition predicted by equilibrium, kinetic, and hybrid approaches are much smaller than those in the HK and TB cases, indicating that the aerosol sample collected in Angiola is close to equilibrium and the bulk equilibrium approaches are adequate for this test case.

3.2. Computational Cost of Schemes

[31] Table 4 shows the CPU times per simulation hour averaged based on simulations for the HK, TB, and CRPAQS/AN cases. All the simulations are conducted on dual Xeon computer nodes with 2.8–3.2 GHz Intel Xeon Processors, 4-GB memory on an IBM Blade Center Linux Cluster at North Carolina State University. As expected, the bulk equilibrium approach is most computationally efficient. Since the Walcek scheme requires a small time step, it is the slowest scheme among all approaches tested here. The CPU time for the 8-bin kinetic/APC_MC scheme with the same time step as kinetic/Walcek (i.e., 0.5 s) is 1.8 s, which is close to that (2.2 s) used by the 8-bin kinetic/Walcek scheme. With a time step of 15 s, the 8-bin kinetic/APC_MC scheme becomes much faster (i.e., 0.11 s). Since the modified CMU hybrid/APC_MC approach uses the bulk

Figure 11. Initial size-resolved aerosol composition on 17 December 2000 and simulated composition on 18 December 2000 by the equilibrium, kinetic, and hybrid approaches in box MADRID with 8 sections ((a)–(f)) and that by the kinetic approaches with 500 sections ((g)–(h)) in Angiola. The measured size-resolved aerosol composition on 18 December is also shown in Figure 11i. The results from the 500-section kinetic approaches are aggregated into 8 sections.

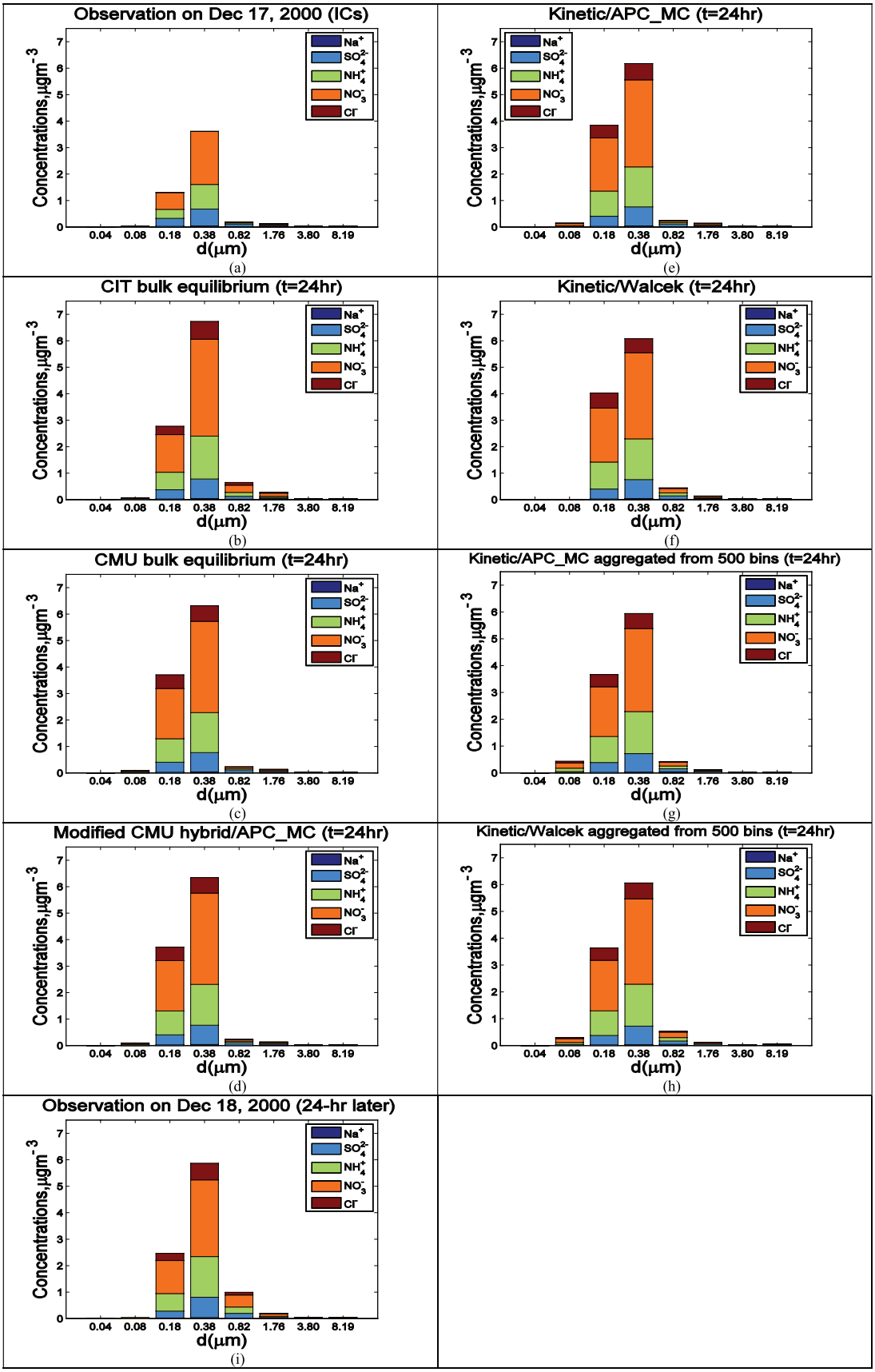
Observation on Dec 17, 2000 (ICs)
(a)
Kinetic/APC_MC (t=24hr)
(e)
CIT bulk equilibrium (t=24hr)
(b)
Kinetic/Walcek (t=24hr)
(f)
CMU bulk equilibrium (t=24hr)
(c)
Kinetic/APC_MC aggregated from 500 bins (t=24hr)
(g)
Modified CMU hybrid/APC_MC (t=24hr)
(d)
Kinetic/Walcek aggregated from 500 bins (t=24hr)
(h)
Observation on Dec 18, 2000 (24-hr later)
(i)
Concentrations,μgm-3
d(μm)
0.04 0.08 0.18 0.38 0.82 1.76 3.80 8.19
Na+
SO4 2-
NH4+
NO3-
Cl-

Figure 11

Table 4. CPU Time Per Simulation Hour and Time Step Used for Different Gas/Particle Mass Transfer Approaches in the Box MADRID Test Simulations

Number of Bins	8-Bin						500-Bin	
	Equilibrium		Kinetic			Modified CMU	Kinetic	
Approach	CIT	CMU	APC_MC		Walcek	Hybrid/APC_MC	APC_MC	Walcek
CPU time, s	0.03	0.03	0.11	1.8	2.2	0.06	115.9	133.7
Time step used, s	60	60	15	0.5	0.5	60 for equilibrium calculation; 15 for kinetic calculation	0.5	0.5

equilibrium approach for the first 6 sections, it costs about half of the CPU time of the 8-bin kinetic/APC_MC approach (0.06 s). The ability to use larger time steps while maintaining the accuracy makes both the kinetic/APC_MC and the modified CMU hybrid/APC_MC approaches attractive for their 3-D applications.

4. Summary

[32] Three gas/particle mass transfer approaches (i.e., bulk equilibrium, kinetic, and hybrid) and five condensation/evaporation schemes (e.g., the Bott, T-G, Walcek, APC_MC, and APC_FM schemes) are evaluated using benchmarks with a high size resolution and a small time step and available observations. In the condensation-only test with a hypothetical case, the APC_FM, APC_MC, and Walcek schemes are more accurate than the Bott and T-G schemes. The original formulation of the Bott scheme as implemented in several PM air quality models is subject to upstream diffusion; it does not warrant its continuous use without modifications for simulating condensation and gas/particle mass transfer in air quality models. By increasing the size resolution for the APC_FM scheme and both the size and pulse resolutions for the T-G scheme, its performance can be greatly improved. The box MADRID tests for gas/particle mass transfer approaches are conducted using observations from three distinct sets of size-distributed particle chemical composition and concurrent gas species and meteorological data obtained in HK, TB, and CRPAQS/AN. Observations and benchmark results are used to evaluate performance of various approaches for all three cases except for the TB case where observations after 48-h simulation are not available. For HK and TB cases with high nitrate in the coarse mode, bulk equilibrium approaches fail to predict the distribution of semivolatile species (e.g., NH_4^+, Cl^-, and NO_3^-) when the observed aerosol is not in an equilibrium state and the compositions of different sections are different due to its inherent weaknesses: assuming an instantaneous equilibrium between bulk gas and liquid/solid phases and internal mixture across all the sections. The CMU hybrid approach also has a similar problem but to a lesser extent for some cases since it assumes bulk equilibrium for fine size sections, although it is considered to be reasonably accurate. The kinetic approaches (including the kinetic/APC_MC and kinetic/Walcek schemes) predict the most accurate solutions for the HK case as compared with observations and the benchmarks. For the TB case, the modified CMU hybrid/APC_MC, kinetic/APC_MC, and kinetic/Walcek approaches predict the closest distributions to the benchmarks, although the resulting size distributions for chloride simulated by all approaches significantly deviate from its initial distribution, resulting from a lack of treatment for crustal species in the aerosol thermodynamic calculation in the box MADRID under such conditions. For the CRPAQS/AN case with all nitrate in the fine mode, the bulk equilibrium approach predicts a similar size distribution to that of the kinetic and hybrid approaches since the aerosol sample is close to equilibrium. The performance of all approaches against observations and benchmarks is quite similar.

[33] Among all approaches tested, the bulk equilibrium approach is most computationally efficient. The kinetic/Walcek scheme provides an accurate solution but is the slowest due to its requirement for a small time step. The kinetic/APC_MC and modified CMU hybrid/APC_MC schemes appear to be attractive for 3-D applications by providing the best compromise between accuracy and computational efficiency. MADRID has been incorporated into an advanced 3-D Weather Research and Forecast/Chemistry Model (WRF/Chem) (referred to as WRF/Chem-MADRID) [*Zhang et al.*, 2005; *Hu and Zhang*, 2006]. Simulations with the CIT bulk equilibrium, the modified CMU hybrid/APC_MC scheme, and the kinetic/APC_MC schemes are being conducted using WRF/Chem-MADRID [*Hu et al.*, 2006; *Hu and Zhang*, 2007] to further evaluate the performance of those schemes in the presence of other processes such as transport and removal. Such 3-D model simulations will provide an assessment of their performance in real atmosphere and will be presented in a future paper.

[34] **Acknowledgments.** This work was performed at NCSU under the Memorandum of Understanding between the U.S. Environmental Protection Agency (EPA) and the U.S. Department of Commerce's National Oceanic and Atmospheric Administration (NOAA) and under agreement number DW13921548, funding under the NOAA Air Quality Forecast Fellowship Program within University Corporation for Atmospheric Research (UCAR)'s Visiting Scientist Program and the NOAA Faculty Research Participation Program of the Oak Ridge Institute for Science and Education (ORISE), and the National Science Foundation Career Award No. Atm-0348819, and was funded, in part, at Stanford University under the NOAA Contract No. NMRAC200540009. Thanks are due to David Chock, Ford Research Laboratory and Chris J. Walcek, the State University of New York at Albany, for providing the FORTRAN codes for the T-G and the Walcek schemes, respectively. Thanks are also due to Shaocai Yu, the U.S. NOAA/EPA, for providing PM data at Tampa, FL, and Gregory O'Brien, Jinyou Liang, and Karen Magliano, California Air Resources Board, for providing the CRPAQS observational data. The authors also gratefully acknowledge the NOAA Air Resources Laboratory (ARL) for the provision of the HYSPLIT transport and dispersion model and/or READY website (http://www.arl.noaa.gov/ready.html) used in this work. Thanks are also due to three anonymous reviewers, who provided constructive comments during the revision of the manuscript.

References

Ackermann, I. J., H. Hass, M. Memmesheimer, A. Ebel, F. S. Binkowski, and U. Shankar (1998), Modal aerosol dynamics model for Europe: Development and first applications, *Atmos. Environ.*, *32*, 2981–2999.

Ansari, A. S., and S. N. Pandis (1999), An analysis of four models predicting the partitioning of semi-volatile inorganic aerosol components, *Aerosol Sci. Technol.*, *31*, 129–153.

Baek, B. H., V. P. Aneja, and Q. Tong (2004), Chemical coupling between ammonia, acid gases, and fine particles, *Environ. Pollut.*, *129*, 89–98.

Binkowski, F. S., and S. J. Roselle (2003), Models-3 community multiscale air quality (CMAQ) model aerosol component: 1. Model description, *J. Geophys. Res.*, *108*(D6), 4183, doi:10.1029/2001JD001409.

Binkowski, F. S., and U. Shankar (1995), The regional particulate matter model: 1. Model description and preliminary results, *J. Geophys. Res.*, *100*, 26,191–26,209.

Bott, A. (1989), A positive definite advection scheme obtained by nonlinear renormalization of the advective fluxes, *Mon. Weather Rev.*, *117*, 1006–1015.

Campbell, S. W., M. C. Evans, and N. D. Poor (2002), Predictions of size-resolved aerosol concentrations of ammonium, chloride and nitrate at a bayside site using EQUISOLV II, *Atmos. Environ.*, *36*, 4299–4307.

Capaldo, K. P., C. Pilinis, and S. N. Pandis (2000), A computationally efficient hybrid approach for dynamic gas/aerosol transfer in air quality models, *Atmos. Environ.*, *34*, 3617–3627.

Chock, D. P., P. Sun, and S. L. Winkler (1996), Trajectory-grid: An accurate sign-preserving advection-diffusion approach for air quality modeling, *Atmos. Environ.*, *30*(6), 857–868.

Chock, D. P., and S. L. Winkler (2000), A trajectory-grid approach for solving the condensation and evaporation equations of aerosols, *Atmos. Environ.*, *34*, 2957–2973.

Chock, D. P., M. J. Whalen, S. L. Winkler, and P. Sun (2005), Implementing the trajectory-grid transport algorithm in an air quality model, *Atmos. Environ.*, *39*(22), 4015–4023.

Chow, J. C., L.-W. A. Chen, J. G. Watson, D. H. Lowenthal, K. A. Magliano, K. Turkiewicz, and D. E. Lehrman (2006a), $PM_{2.5}$ chemical composition and spatiotemporal variability during the California Regional $PM_{10}/PM_{2.5}$ Air Quality Study (CRPAQS), *J. Geophys. Res.*, *111*, D10S04, doi:10.1029/2005JD006457.

Chow, J. C., J. G. Watson, D. H. Lowenthal, L. W. A. Chen, R. J. Tropp, K. Park, and K. Magliano (2006b), $PM_{2.5}$ and PM_{10} mass measurements in California's San Joaquin Valley, *Aerosol Sci. Technol.*, *40*(10), 796–810.

Debry, E., K. Fahey, K. Sartelet, B. Sportisse, and M. Tombette (2007), Technical note: A new Size Resolved Aerosol Model (SIREAM), *Atmos. Chem. Phys.*, *7*, 1537–1547.

Dasgupta, P. K., S. W. Campbell, R. S. Al-Horr, S. M. R. Ullah, J. Li, C. Amalfitano, and N. D. Poor (2007), Conversion of sea salt aerosol to NaNO3 and the production of HCl: Analysis of temporal behavior of aerosol chloride/nitrate and gaseous HCl/HNO_3 concentrations with AIM, *Atmos. Environ.*, *41*(20), 4242–4257.

Dhaniyala, S., and A. S. Wexler (1996), Numerical schemes to model condensation and evaporation of aerosols, *Atmos. Environ.*, *30*(6), 919–928.

Draxler, R. R., and G. D. Rolph (2003), HYSPLIT (HYbrid Single-Particle Lagrangian Integrated Trajectory) model access via NOAA ARL READY Website (http://www.arl.noaa.gov/ready/hysplit4.html), NOAA Air Resources Laboratory, Silver Spring, Md.

Evans, M., and N. D. Poor (2001), Scrubbing of atmospheric nitric acid and sulfuric acid by marine air, Paper 521, in *Proc. 94th Annual Air Waste Manage. Conf. Exhib.*, 24–28 June, Orlando, Fla., A&WMA, Pittsburg, Pa.

Evans, M. C., S. W. Campbell, V. Bhethanabotla, and N. D. Poor (2004), Effect of sea salt and calcium carbonate interactions with nitric acid on the direct dry deposition of nitrogen to Tampa Bay, *Atmos. Environ.*, *38*(29), 4847–4858.

Fridlind, A. M., and M. Z. Jacobson (2000), A study of gas-aerosol equilibrium and aerosol pH in the remote marine boundary layer during the first aerosol characterization experiment (ACE-1), *J. Geophys. Res.*, *105*, 17325–17340.

Fridlind, A. M., M. Z. Jacobson, V.-M. Kerminen, R. E. Hillamo, V. Ricard, and J.-L. Jaffrezo (2000), Analysis of gas-aerosol partitioning in the Arctic: Comparison of size-resolved equilibrium model results with field data, *J. Geophys. Res.*, *105*, 19,891–19,904.

Gaydos, T. M., B. Koo, S. N. Pandis, and D. P. Chock (2003), Development and application of an efficient moving sectional approach for the solution of the atmospheric aerosol condensation/evaporation equations, *Atmos. Environ.*, *37*, 3303–3316.

Gaydos, T. M., R. Pinder, B. Koo, K. M. Fahey, G. Yarwood, and S. N. Pandis (2007), Development and application of a three-dimensional aerosol chemical transport model, PMCAMx, *Atmos. Environ.*, *41*, 2594–2611.

Goetz, S., V. Aneja, and Y. Zhang (2008), Measurement, analysis, and modeling of fine particulate matter in Eastern North Carolina, *J. Air Waste Manage. Assoc.*, in press.

Hayami, H., and G. R. Carmichael (1997), Analysis of aerosol composition at Cheju Island, Korea, using a two-bin gas-aerosol equilibrium model, *Atmos. Environ.*, *31*, 3429–3439.

Hu, X.-M., Y. Zhang, and M. Z. Jacobson (2005), Evaluation of the trajectory-grid and the Bott schemes for solving aerosol condensation and evaporation equations, in *Proc. 4th Ann. CMAS Models-3 User's Conf.*, 26–28 September, Chapel Hill, N. C.

Hu, X.-M., and Y. Zhang (2006), Implementation and testing of a new aerosol module in WRF/chem, in *Proc. 86th AMS Annual Meeting/the 8th Conf. Atmos. Chem.*, 27 Jan.–3 Feb., Atlanta, Ga.

Hu, X.-M., Y. Zhang, and M. Z. Jacobson (2006), Evaluation and improvement of gas/particle mass transfer treatments for three-dimensional aerosol simulation and forecast, in *Proc. 5th Ann. CMAS Models-3 User's Conf.*, 16–18 October, Chapel Hill, N. C.

Hu, X.-M., and Y. Zhang (2007), Gas/particle mass transfer treatments in WRF/Chem-MADRID: Development, application, and evaluation, presentation at the *8th Annual WRF User's Workshop*, 11–15 June, Boulder, Colo.

Jacobson, M. Z. (1995), Computation of global photochemistry with SMVGEAR II, *Atmos. Environ.*, *29A*, 2541–2546.

Jacobson, M. Z. (1997a), Development and application of a new air pollution modeling system. Part II: Aerosol module structure and design, *Atmos. Environ.*, *31*, 131–144.

Jacobson, M. Z. (1997b), Numerical techniques to solve condensational and dissolutional growth equations when growth is coupled to reversible reactions, *Aerosol Sci. Technol.*, *27*, 491–498.

Jacobson, M. Z. (1999), Studying the effects of calcium and magnesium on size-distributed nitrate and ammonium with EQUISOLV II, *Atmos. Environ.*, *33*, 3635–3649.

Jacobson, M. Z. (2005), A solution to the problem of nonequilibrium acid/base gas-particle transfer at long time step, *Aerosol Sci. Technol.*, *39*, 92–103.

Kerminen, V.-M., R. Hillamo, K. Teinilä, T. Pakkanen, I. Allegrini, and R. Sparapani (2001), Ion balances of size-resolved tropospheric aerosol samples: Implications for the acidity and atmospheric processing of aerosols, *Atmos. Environ.*, *35*, 5255–5265.

Koo, B., T. M. Gaydos, and S. N. Pandis (2003), Evaluation of the equilibrium, dynamic, and hybrid aerosol modeling approaches, *Aerosol Sci. Technol.*, *37*, 53–64.

Louie, P. K. K., J. G. Watson, J. C. Chow, A. Chen, D. W. M. Sin, and A. K. H. Lau (2005), Seasonal characteristics and regional transport of $PM_{2.5}$ in Hong Kong, *Atmos. Environ.*, *39*, 1695–1710.

Lurmann, F. W., A. S. Wexler, S. N. Pandis, S. Musarra, N. Kumar, and J. H. Seinfeld (1997), Modeling urban and regional aerosols. Part II. Application to California's South Coast air basin, *Atmos. Environ.*, *31*, 2695–2715.

Magliano, K. L., V. M. Hughes, L. R. Chinkin, D. L. Coe, T. L. Haste, N. Kumar, and F. W. Lurmann (1999), Spatial and temporal variations in PM_{10} and $PM_{2.5}$ source contributions and comparison to emissions during the 1995 integrated monitoring study, *Atmos. Environ.*, *33*(29), 4757–4773.

McDade, C. E. (2002), California Regional PM10/PM2.5 Air Quality Study (CRPAQS) Introduction to Site Documentation Reports. California Regional PM10/PM2.5 Air Quality Study Technical Committee c/o California Air Resources Board Sacramento CA. by ENSR International Camarillo, CA.

Meng, Z., and J. H. Seinfeld (1996), Time scales to achieve atmospheric gas-aerosol equilibrium for volatile species, *Atmos. Environ.*, *30*, 2889–2900.

Meng, Z., D. Dabdub, and J. H. Seinfeld (1998), Size-resolved and chemically resolved model of atmospheric aerosol Dynamics, *J. Geophys. Res.*, *103*, 3419–3435.

Metzger, S., F. Dentener, S. Pandis, and J. Levieveld (2002), Gas/aerosol partitioning: 1. A computationally efficient model, *J. Geophys. Res.*, *107*(D16), 4312, doi:10.1029/2001JD001102.

Moya, M., A. S. Ansari, and S. N. Pandis (2001), Partitioning of nitrate and ammonium between the gas and particulate phases during the 1997 IMADA-AVER study in Mexico City, *Atmos. Environ.*, *35*, 1791–1804.

Moya, M., S. Pandis, and M. Jacobson (2002), Is the size distribution of urban aerosols determined by thermodynamic equilibrium? An application to southern California, *Atmos. Environ.*, *36*(14), 2349–2365.

Moya, M., T. Castro, M. Zepeda, and A. Baez (2003), Characterization of size-differentiated inorganic composition of aerosols in Mexico City, *Atmos. Environ.*, *37*, 3581–3591.

Myhre, G., A. Grini, and S. Metzger (2006), Modelling of nitrate and ammonium-containing aerosols in presence of sea salt, *Atmos. Chem. Phys.*, *6*, 4809–4821.

Nenes, A., C. Pilinis, and S. N. Pandis (1998), ISORROPIA: A new thermodynamic equilibrium model for multiphase multicomponent marine aerosols, *Aquat. Geochem.*, *4*, 123–152.

Nenes, A., C. Pilinis, and S. N. Pandis (1999), Continued development and testing of a new thermodynamic aerosol module for urban and regional air quality models, *Atmos. Environ.*, *33*, 1553–1560.

Nguyen, K., and D. Dabdub (2002), Semi-Langrangian flux scheme for the solution of the aerosol condensation/evaporation equation, *Aerosol Sci. Technol.*, *36*(4), 407–418.

Pandis, S. N., A. S. Wexler, and J. H. Seinfeld (1993), Secondary organic aerosol formation and transport. Part II: Predicting the ambient secondary organic aerosol size distribution, *Atmos. Environ.*, *27A*, 2403–2416.

Pathak, R. K., X. H. Yao, A. K. H. Lau, and C. K. Chan (2003), Acidity and concentrations of ionic species of $PM_{2.5}$ in Hong Kong, *Atmos. Environ.*, *37*, 1113–1124.

Pathak, R. K., X. H. Yao, and C. K. Chan (2004), Sampling artifacts of acidity and ionic species in $PM_{2.5}$, *Environ. Sci. Technol.*, *38*, 254–259.

Pilinis, C., and J. H. Seinfeld (1987), Continued development of a general equilibrium model for inorganic multicomponent atmospheric aerosols, *Atmos. Environ.*, *21*(11), 2453–2466.

Pilinis, C., J. H. Seinfeld, and C. Seigneur (1987), Mathematical modeling of the dynamics of multicomponent atmospheric aerosols, *Atmos. Environ.*, *21*, 943–955.

Pilinis, C., K. P. Capaldo, A. Nenes, and S. N. Pandis (2000), MADM-A new multicomponent aerosol dynamics model, *Aerosol Sci. Technol.*, *32*, 482–502.

Plessow, K., G. Spindler, F. Zimmermann, and J. Matschullat (2005), Seasonal variations and interactions of N-containing gases and particles over a coniferous forest, Saxony, Germany, *Atmos. Environ.*, *39*, 6995–7007.

Poor, N., R. Pribble, and H. Greening (2001), Direct wet and dry deposition of ammonia, nitric acid, ammonium and nitrate to the Tampa Bay Estuary, FL, USA, *Atmos. Environ.*, *35*, 3947–3955.

Pun, B. K., and C. Seigneur (1999), Understanding particulate matter formation in the California San Joaquin Valley: Conceptual model and data needs, *Atmos. Environ.*, *33*, 4865–4875.

Russell, A. G., G. J. McRae, and G. R. Cass (1983), Mathematical modeling of the formation and transport of ammonium nitrate aerosol, *Atmos. Environ.*, *17*, 949–965.

Russell, A. G., K. F. McCue, and G. R. Cass (1988), Mathematical modeling of the formation of nitrogen-containing air pollutants. Part I: Evaluation of an Eulerian photochemical model, *Environ. Sci. Technol.*, *22*, 263–271.

Russell, A. G., D. A. Winner, R. A. Harley, K. F. McCue, and G. R. Cass (1993), Mathematical modeling and control of the dry deposition flux of nitrogen-containing air pollutants, *Environ. Sci. Technol.*, *27*, 2772–2782.

Seigneur, C., A. B. Hudischewskyi, J. H. Seinfeld, K. T. Whitby, E. R. Whitby, J. R. Brock, and H. M. Barnes (1986), Simulation of aerosol dynamics: A comparative review of mathematical models, *Aerosol Sci. Technol.*, *5*, 205–222.

Seigneur, C. (2001), Current status of air quality modeling for particulate matter, *J. Air Waste Manage. Assoc.*, *51*, 1508–1521.

Seinfeld, J. H. and S. N. Pandis (1998). *Atmospheric Chemistry and Physics: From Air Pollution to Climate Change*, Wiley, New York.

Sun, Q., and A. S. Wexler (1998), Modeling urban and regional aerosols - Condensation and evaporation near acid neutrality, *Atmos. Environ.*, *32*, 3527–3531.

Tombette, M., and B. Sportisse (2007), Aerosol modeling at a regional scale: Model-to-data comparison and sensitivity analysis over Greater Paris, *Atmos. Environ.*, doi:10.1016/j.atmosenv.2006.10.037.

Trebs, I., et al. (2005), The NH_4^+–NO_3^- – Cl^-–SO_4^{2-}–H_2O aerosol system and its gas phase precursors at a pasture site in the Amazon Basin: How relevant are mineral cations and soluble organic acids?, *J. Geophys. Res.*, *110*, D07303, doi:10.1029/2004JD005478.

Walcek, C. J., and N. M. Aleksic (1998), A simple but accurate mass conservative, peak-preserving, mixing ratio bounded advection algorithm with FORTRAN code, *Atmos. Environ.*, *32*, 3863–3880.

Walcek, C. J. (2000), Minor flux adjustment near mixing ratio extremes for simplified yet highly accurate monotonic calculation of tracer advection, *J. Geophys. Res.*, *105*, 9335–9348.

Watson, J. G., J. C. Chow, L.-W. A. Chen, L. Rinehart, and B. Zielinska (2005), Spatial variability of $PM_{2.5}$ species in the California Central Valley, presented at the *AAAR International Specialty Conference*, Atlanta, Ga., 8 February.

Wang, K., Y. Zhang, M. Z. Jacobson, J.-Y. Liang, and K. Magliano (2006), A study of gas/particle partitioning using inorganic thermodynamic equilibrium modules and data from the California regional PM_{10}/$PM_{2.5}$ air quality study, in *Proc. Workshop on Agricultural Air Quality: State of the Science*, 5–8 June, Potomac, Md.

Wexler, A. S., and J. H. Seinfeld (1990), The distribution of ammonium salts among a size and composition dispersed aerosol, *Atmos. Environ.*, *24A*, 1231–1246.

Wexler, A. S., F. W. Lurmann, and J. H. Seinfeld (1994), Modeling urban and regional aerosols. Part I: Model development, *Atmos. Environ.*, *28*(3), 531–546.

Yao, X. H., M. Fang, and C. K. Chan (2001), Experimental study of the sampling artifact of chloride depletion from collected sea salt aerosols, *Environ. Sci. Technol.*, *35*, 600–605.

Yao, X. H., T. Y. Ling, M. Fang, and C. K. Chan (2006), Comparison of thermodynamic predictions for in-situ pH in $PM_{2.5}$, *Atmos. Environ.*, *40*, 2835–2844.

Yao, X. H., T. Y. Ling, M. Fang, and C. K. Chan (2007), Size dependence of in situ pH in submicron atmospheric particles in Hong Kong, *Atmos. Environ.*, *41*, 382–393.

Zhang, Y., C. Seigneur, J. H. Seinfeld, M. Jacobson, and F. S. Binkowski (1999), Simulation of aerosol dynamics: A comparative review of algorithms used in air quality models, *Aerosol Sci. Technol.*, *31*(6), 487–514.

Zhang, J., W. L. Chameides, R. J. Weber, G. Cass, D. Orsini, E. Edgerton, P. Jongejan, and J. Slanina (2002), An evaluation of the thermodynamic equilibrium assumption for fine particulate composition: Nitrate and ammonium during the 1999 Atlanta supersite experiment, *J. Geophys. Res.*, *108*(D7), 8414, doi:10.1029/2001JD001592.

Zhang, Y., B. Pun, K. Vijayaraghavan, S.-Y. Wu, C. Seigneur, S. Pandis, M. Jacobson, A. Nenes, and J. H. Seinfeld (2004), Development and application of the model of aerosol dynamics, reaction, ionization and dissolution (MADRID), *J. Geophys. Res.*, *109*, D01202, doi:10.1029/2003JD003501.

Zhang, Y., X.-M. Hu, G. W. Howell, E. Sills, J. D. Fast, W. I. Gustafson Jr., R.A. Zaveri, G. A. Grell, S. E. Peckham, and S. A. McKeen (2005), Modeling atmospheric aerosols in WRF/CHEM, in *Proc. 2005 Joint WRF/MM5 User's Workshop*, 27–30 June, Boulder, Colo.

Zhuang, H., C. K. Chan, M. Fang, and A. S. Wexler (1999a), Size distributions of particulate sulfate, nitrate and ammonium at a coastal site in Hong Kong, *Atmos. Environ.*, *33*, 843–853.

Zhuang, H., C. K. Chan, M. Fang, and A. S. Wexler (1999b), Formation of nitrate and non-sea-salt sulfate on coarse particles, *Atmos. Environ.*, *33*, 4223–4233.

C. K. Chan, Department of Chemical Engineering, Rm. 4559, Lift 27 and 28, Hongkong University of Science and Technology, Clear Water Bay, Kowloon, Hongkong.

X.-M. Hu and Y. Zhang, Department of Marine, Earth and Atmospheric Sciences, North Carolina State University, 1125 Jordan Hall, Campus Box 8208, 2800 Faucette Drive Raleigh, NC 27695, USA. (yzhang9@ncsu.edu)

M. Z. Jacobson, Department of Civil and Environmental Engineering, Stanford University, Yang and Yamazaki Environment and Energy Bldg., 473 Via Ortega, Room 397, Stanford, CA 94305-4020, USA.